Plant Physiology Preview. Published on July 28, 2015, as DOI:10.1104/pp.15.00851

RUNNING HEAD: Galactoglucomannan Maintains Mucilage Architecture

Cătălin Voiniciuc

Institute for Bio- and Geosciences (IBG-2: Plant Sciences), Forschungszentrum Jülich, 52425 Jülich, Germany

+49 (0)2461 61 3465

c.voiniciuc@fz-juelich.de

RESEARCH AREA: Biochemistry and Metabolism

Copyright 2015 by the American Society of Plant Biologists

MUCI10 Produces Galactoglucomannan That Maintains Pectin and Cellulose Architecture in Arabidopsis Seed Mucilage

Cătălin Voiniciuc*, Maximilian Heinrich-Wilhelm Schmidt, Adeline Berger, Bo Yang, Berit Ebert, Henrik V. Scheller, Helen M. North, Björn Usadel and Markus Günl

Institute for Bio- and Geosciences (IBG-2: Plant Sciences), Forschungszentrum Jülich, 52425 Jülich, Germany (C.V, M.H.-W.S., M.G., B.U.); Institute for Botany and Molecular Genetics (IBMG), BioEconomy Science Center, RWTH Aachen University, 52056 Aachen, Germany (C.V., M.H.-W.S, B.Y., B.U.); INRA, Institut Jean-Pierre Bourgin, UMR1318, ERL CNRS 3559, Saclay Plant Sciences, RD10, F-78026 Versailles, France (A.B., H.M.N.); AgroParisTech, Institut Jean- Pierre Bourgin, UMR1318, ERL CNRS 3559, Saclay Plant Sciences, RD10, F-78026 Versailles, France (A.B., H.M.N.); Joint BioEnergy Institute and Physical Biosciences Division, Lawrence Berkeley National Laboratory, Berkeley, CA 94702 (B.E., H.V.S.); Department of Plant and Microbial Biology, University of California, Berkeley, CA 94720 (H.V.S.)

E-Mails: c.voiniciuc@fz-juelich.de (C.V.); m.schmidt@fz-juelich.de (M.H.-W.S); adeline.berger@versailles.inra.fr (A.B.); yang@bio1.rwth-aachen.de (B.Y.); bebert@lbl.gov (B.E.); hscheller@lbl.gov (H.S.V); helen.north@versailles.inra.fr (H.M.N.); usadel@bio1.rwth-aachen.de (B.U.); m.guenl@fz-juelich.de (M.G.)

* Address correspondence to c.voiniciuc@fz-juelich.de

The author responsible for distribution of materials integral to the findings presented in this article in accordance with the policy described in the Instructions for Authors (www.plantphysiol.org) is: Cătălin Voiniciuc (c.voiniciuc@fz-juelich.de).

One-Sentence Summary:

MUCI10 decorates glucomannan synthesized by CSLA2 to produce a highly branched polymer that defines the distribution of pectin and the structure of cellulose in Arabidopsis mucilage.

FOOTNOTES:

The research of C.V. was supported in part by the Natural Sciences and Engineering Research Council of Canada (NSERC PGS-D3), and by a travel grant from Saclay Plant Sciences. The scientific activities of M.H.-W.S. and B.U. in the BioEconomy Science Center were financially supported by the Ministry of Innovation, Science and Research of North-Rhine Westphalia, within the framework of the NRW Strategieprojekt BioSC (No. 313/323-400-00213). B.Y. was partly supported by the China Scholarship Council (CSC, No. 201206760005).

ABSTRACT

Plants invest a lot of their resources into the production of an extracellular matrix built of polysaccharides. While the composition of the cell wall is relatively well characterized, the functions of the individual polymers and the enzymes that catalyze their biosynthesis remain poorly understood. We exploited the *Arabidopsis thaliana* seed coat epidermis (SCE) to study cell wall synthesis. SCE cells produce mucilage, a specialized secondary wall that is rich in pectin, at a precise stage of development. A co-expression search for *MUCILAGE-RELATED* (*MUCI*) genes identified *MUCI10* as a key determinant of mucilage properties. MUCI10, a member of the GT34 family, is closely related to a fenugreek enzyme that has *in vitro* galactomannan α-1,6-galactosyltransferase activity. Our detailed analysis of the *muci10* mutants demonstrates that mucilage contains highly branched galactoglucomannan (GGM) rather than unbranched glucomannan. MUCI10 likely decorates glucomannan, synthesized by CSLA2, with galactose residues *in vivo*. The degree of galactosylation is essential for the synthesis of the GGM backbone, the structure of cellulose, mucilage density, as well as the adherence of pectin. We propose that GGM scaffolds control mucilage architecture along with cellulosic rays, and show that Arabidopsis SCE cells represent an excellent model to study the synthesis and function of GGM. Arabidopsis natural varieties with defects similar to *muci10* mutants may reveal additional genes involved in GGM synthesis. Since GGM is the most abundant hemicellulose in the secondary walls of gymnosperms, understanding its biosynthesis may facilitate improvements in the production of valuable commodities from softwoods.

INTRODUCTION

The plant cell wall is the key determinant of plant growth (Cosgrove, 2005), and represents the most abundant source of biopolymers on the planet (Pauly and Keegstra, 2010). Consequently, plants invest a lot of their resources into the production of this extracellular structure. Thus it is not surprising that around 15% of *Arabidopsis thaliana* (Arabidopsis) genes are likely dedicated to the biosynthesis and modification of cell wall polymers (Carpita et al., 2001). Plant walls consist mainly of polysaccharides (cellulose, hemicellulose, and pectin), but also contain lignin and glycoproteins. While the biochemical structure of each wall component has been relatively well characterized, the molecular players involved in their biogenesis remain poorly understood (Keegstra, 2010). The functions of the individual polymers, and how they are assembled into a three-dimensional matrix are also largely unknown (Burton et al., 2010; Burton and Fincher, 2012).

Significant breakthroughs in cell wall research have been achieved through examination of specialized plant tissues that contain elevated levels of a single polysaccharide (Pauly and Keegstra, 2010). Some species, particularly legumes, accumulate large amounts of the hemicellulose galactomannan during secondary wall thickening of the seed (Srivastava and Kapoor, 2005). Analysis of the developing fenugreek (*Trigonella foenumgraecum*) endosperm led to purification of a GALACTOMANNAN GALACTOSYLTRANSFERASE (TfGMGT), the first glycosyltransferase (GT) whose activity in plant cell wall synthesis was demonstrated *in vitro* (Scheller and Ulvskov, 2010). TfGMGT catalyzes the decoration of mannan chains with single α-1,6-galactosyl residues (Edwards et al., 1999). A similar approach in guar (*Cyamopsis tetragonoloba*) seeds revealed that the β-1,4-linked mannan backbone is synthesized by a member of the CELLULOSE SYNTHASE-LIKE A (CSLA) protein family (Dhugga et al., 2004).

Galactomannan functions as storage polymer in the endosperm of the aforementioned seeds, analogous to starch in cereal grains (Dhugga et al., 2004), but it also has important rheological properties in the cell wall that have been exploited to produce valuable stabilizers and gelling agents for human consumption (Srivastava and Kapoor, 2005). The mannose (Man) to galactose (Gal) ratio is essential for the application of galactomannan gums in the food industry (Edwards et al., 1992). This is because unsubstituted mannan chains can interact via hydrogen bonds to produce crystalline microfibrils similar to cellulose (Millane and Hendrixson, 1994). Indeed, some algae that lack cellulose employ mannan fibrils as a structural material (Preston, 1968). The addition of Gal branches to the “smooth”, ribbon-like mannan chains

creates “hairy” regions that limit self-association and promote gelation (Dea et al., 1977). All mannans are likely synthesized as highly substituted polymers that are trimmed in the cell wall (Scheller and Ulvskov, 2010).

Generally, polysaccharides containing backbones of β-1,4-linked Man units can be classified as heteromannan (HM). Galactoglucomannan (GGM) is the main hemicellulose in gymnosperm secondary walls and, in contrast to galactomannan, has a backbone that contains both glucose (Glc) and Man units (Pauly et al., 2013). HM is detected in most Arabidopsis cell types (Handford et al., 2003), and facilitates embryogenesis (Goubet et al., 2009), germination (Rodríguez-Gacio et al., 2012), tip growth (Bernal et al., 2008), and vascular development (Benová-Kákosová et al., 2006; Yin et al., 2011). In the last ten years, *in vitro* mannan synthase activity has been demonstrated for recombinant CSLA proteins from many land plants (Liepman et al., 2005; Suzuki et al., 2006; Liepman et al., 2007; Gille et al., 2011; Wang et al., 2012a). HM synthesis may also involve CELLULOSE SYNTHASE-LIKE D (CSLD) enzymes and MANNAN SYNTHESIS-RELATED (MSR) accessory proteins (Yin et al., 2011; Wang et al., 2012b), but their precise roles in relation to the CSLAs have not been established. Arabidopsis CSLA2, like most other isoforms, can use both GDP-Man and GDP-Glc as substrates *in vitro* (Liepman et al., 2005; Liepman et al., 2007), and is responsible for stem glucomannan synthesis *in vivo* along with CSLA3 and CSLA7 (Goubet et al., 2009). CSLA2 also participates in the synthesis of glucomannan present in mucilage produced by seed coat epidermal (SCE) cells (Yu et al., 2014).

Arabidopsis SCE cells represent an excellent genetic model to study the synthesis, polar secretion and modification of polysaccharides, since these processes dominate a precise stage of seed coat development but are not essential for seed viability in lab conditions (Haughn and Western, 2012; North et al., 2014; Voiniciuc et al., 2015). Hydration of mature seeds in water releases a large gelatinous capsule, rich in the pectic polymer rhamnogalacturonan I (RG I), which can be easily stained or extracted (Macquet et al., 2007). Biochemical and cytological experiments indicate that Arabidopsis seed mucilage is more than just pectin and, in addition to cellulose, is likely to contain glycoproteins and at least two hemicellulosic polymers (Voiniciuc et al., 2015). There is mounting evidence that, despite their low abundance, these components play critical functions in seed mucilage architecture. The structure of homogalacturonan (HG), the major pectin in primary cell walls, but a minor mucilage component, appears to be a key determinant of gelling properties and mucilage extrusion (Rautengarten et al., 2008; Saez-Aguayo et al., 2013; Voiniciuc et al., 2013). Mucilage attachment to seeds is maintained by the SOS5 glycoprotein and cellulose synthesized by multiple CELLULOSE SYNTHASE (CESA)

isoforms (Harpaz-Saad et al., 2011; Mendu et al., 2011; Sullivan et al., 2011; Griffiths et al., 2014; Griffiths et al., 2015). From more than 35 genes that are reported to affect Arabidopsis seed mucilage properties (Voiniciuc et al., 2015), only *CSLA2*, *CESA3*, *CESA5*, *GAUT11* (Caffall et al., 2009), and *GATL5* (Kong et al., 2013), are predicted to encode GTs. This highlights that despite many detailed studies about mucilage production in SCE cells, the synthesis of its components remains poorly understood.

To address this issue, we conducted a reverse genetic search for *MUCILAGE-RELATED* (*MUCI*) genes that may be required for polysaccharide biosynthesis. One of these, *MUCI10*, encodes a member of the Carbohydrate Active Enzymes (CAZy) family GT34 (Lombard et al., 2014), which includes at least two enzymatic activities and seven Arabidopsis proteins (Keegstra and Cavalier, 2010). Five of them function as xyloglucan xylosyltransferases (XXT1 to XXT5) *in vivo* and/or *in vitro* (Faik et al., 2002; Cavalier et al., 2008; Vuttipongchaikij et al., 2012). MUCI10/GT7 (At2g22900) and its paralog GT6 (At4g37690) do not function as XXTs (Vuttipongchaikij et al., 2012), and are more closely related to the TfGMGT enzyme (Faik et al., 2002; Keegstra and Cavalier, 2010). MUCI10, also called GALACTOSYLTRANSFERASE-LIKE6 (GTL6), served as a Golgi marker in multiple proteomic studies of Arabidopsis callus cultures (Dunkley et al., 2004; Dunkley et al., 2006; Nikolovski et al., 2012; Nikolovski et al., 2014). Nevertheless, the role of TfGMGT orthologs in Arabidopsis remained unknown. We show that MUCI10 is responsible for the extensive galactosylation of glucomannan in mucilage, and influences glucomannan backbone synthesis, cellulose structure, and the distribution of pectin.

RESULTS

A *MUCILAGE-RELATED* Screen Yields a *TfGMGT* Ortholog

We used eight known mucilage genes (*MUM4*/*RHM2*, *MUM2*/*BGAL6*, *SBT1.7*/*ARA12*, *PMEI6*, *FLY1*, *BXL1*, *GL2*, *GATL5*), whose seed coat transcript levels are up-regulated during mucilage production (Voiniciuc et al., 2015), as baits in three distinct co-expression tools: GeneCAT, GeneMANIA, and ATTED-II (Mutwil et al., 2008; Warde-Farley et al., 2010; Obayashi et al., 2014). We manually prioritized a total of 600 *MUCI* gene predictions based on three criteria: putative protein function, seed coat expression profile, and the availability of insertion mutants. By screening more than 100 *muci* mutants for altered ruthenium red (RR) mucilage staining, we identified multiple new genes required for polysaccharide synthesis. This study focuses on *MUCI10* and further results of the screen will be described elsewhere.

Both GeneCAT and GeneMANIA predicted that *MUCI10* is involved in mucilage polysaccharide production (Mutwil et al., 2008; Warde-Farley et al., 2010). Indeed, Arabidopsis microarray datasets indicate that *MUCI10* is closely linked to several known mucilage genes, particularly *CSLA2* (Fig. 1A). During seed development, *MUCI10* is specifically expressed in the seed coat, at the linear cotyledon and mature green embryo stages (Supplemental Fig. S1A; Winter et al., 2007; Belmonte et al., 2013). We validated this microarray data using RT-PCR (Fig. 1C), and qRT-PCR (Fig. 1D) analyses of *MUCI10* transcription in developing siliques. *MUCI10* expression increased from the heart to the linear cotyledon stage (Fig 1, C and D), and peaked at the mature green embryo stage (Fig. 1D). *MUCI10* transcripts are 6.2x more abundant in wild-type seed coats at 7 days post-anthesis (DPA; Supplemental Fig. S1B), compared to the *ap2* mutant, which does not produce mucilage (Dean et al., 2011). Similarly, *MUCI10* was expressed five-fold lower in the *knat7-1* mutant (Fig. 1E), which is defective in a transcription factor that was predicted to promote hemicellulose synthesis in seed mucilage (Voiniciuc et al., 2015). In contrast to its paralog, *GT6* does not classify as a *MUCI* gene since it has 1.8x higher expression in *ap2* than in the wild type (Supplemental Fig. S1C; Dean et al., 2011).

To investigate if *MUCI10* and *GT6* are involved in mucilage biosynthesis, we isolated four *muci10* and two *gt6* homozygous insertion mutants (Fig. 1B). The *muci10-1* and *muci10-2* alleles were shown to be transcriptional knockouts (Fig. 1, C and D). Since we detected increased *GT6* transcript levels in *muci10-2* siliques compared to the wild type (Fig. 1C), we generated a *muci10 gt6* double mutant to explore functional redundancy. The *muci10-2 gt6-1* double mutant only had traces of *GT6* transcript similar to the *gt6-1* single mutant, not the elevated levels detected in the *muci10-2* single mutant (Fig. 1C).

Distinct *muci10* and *csla2* Chemical Defects Lead to Equally Compact Mucilage

The seeds of four independent *muci10* alleles were surrounded by smaller mucilage layers than the wild type (Fig. 2). Using Fiji (Schindelin et al., 2012), we developed a simple method that enables the high-throughput quantification of seed and mucilage dimensions (Supplemental Fig. S2). Four *muci10* alleles and the *csla2-3* mutant, which has dense mucilage (Yu et al., 2014), displayed approximately 30% smaller mucilage capsules than the wild type (Fig. 2Q). Two *gt6* alleles showed normal mucilage dimensions, and the *muci10-2 gt6-1* double mutant resembled the *muci10-2* single mutant (Fig. 2). In contrast to their mucilage defects, all mutants had seed areas similar to the wild type (Supplemental Table S1), except for a 6% increase in

gt6-1 (*t*-test, $P < 0.05$). The equally compact mucilage capsules of *muci10* and *csla2* suggested that they may have similar chemical defects.

In mucilage extracted from these two mutants by vigorously shaking seeds in water (Voiniciuc et al., 2015), only three minor sugars (representing 2.5% of mucilage) were significantly altered from the wild type (Table 1). The *muci10-2* and *csla2-3* mutants had equal reductions in Gal, but contained distinct Glc and Man levels (Fig. 2R). The *csla2-3* mutant had ~80% less Man than wild-type mucilage (Table 1), while the *muci10-1*, *muci10-2* and *muci10-3* alleles only had ~50% less Man (Table 1, Supplemental Tables S2 and S3). Given their identical staining and biochemical defects, the first two *muci10* lines were used interchangeably for further experiments. The changes in Gal, Glc and Man content were proportional for each mutant (Fig. 2R). The *csla2-3* mutant lacked around 1.0 nmol of each of these three sugars per mg seed, while *muci10-2* showed reductions of 0.9 nmol Gal, 0.7 nmol Glc and 0.7 nmol Man.

Unlike *MUCI10*, *GT6* Does Not Affect Seed Mucilage Composition

Unlike *muci10* mutants, *gt6-1* and *gt6-2* did not contain reduced Gal, Glc, or Man content in total mucilage (Table 1, Fig. 2R), or non-adherent mucilage extracts (Supplemental Table S3). To test if *GT6* function can compensate partially for *MUCI10* function, we examined the biochemical composition of the *muci10-2 gt6-1* double mutant. The double mutant had a similar composition to the *muci10-2* mutant (Fig. 2R, Table 1). This indicates that *GT6* is not indispensable for the synthesis of mucilage polysaccharides.

MUCI10 Is Necessary For Galactoglucomannan (GGM) Synthesis

To further investigate *MUCI10* function, we analyzed the glycosyl linkages of total mucilage extracts (Table 2), and used these results to calculate the composition of polysaccharides (Fig. 3A). While most polymers had wild-type levels, the *muci10-1* mucilage contained 38% less HM (*t*-test, $P < 0.05$). Unsubstituted glucomannan is the only known HM component of mucilage (Yu et al., 2014), although some of the available linkage data suggests the presence of GGM (Voiniciuc et al., 2015). Lower HM content in *muci10-1* mucilage resulted from reductions in t-Gal, 4-Glc, 4-Man, and 4,6-Man (*t*-test, $P < 0.05$), with 81% less t-Gal as the most severe defect (Table 2, Fig. 3B). The loss of t-Gal correlated with a five-fold decrease in the ratio of branched 4,6-Man to unbranched 4-Man (Fig. 3B). This indicates that *MUCI10* is required for the decoration of glucomannan with t-Gal side chains. Wild-type mucilage contained two branched 2,4-Man residues for every unbranched 4-Man unit (Table 2), suggesting that GGM rather than

unbranched glucomannan is the most abundant Man-containing polymer in mucilage. This model was also supported by an enzyme-linked immunosorbent assay (ELISA) of total mucilage extracts using LM22 (Fig. 3C), a monoclonal antibody that only effectively binds HM polymers without Gal side chains (Marcus et al., 2010). Relative to wild-type mucilage, *muci10-1* contained significantly more non-galactosylated HM, while *csla2-3* contained significantly fewer LM22 epitopes (Fig. 3C). These results indicate that mucilage contains GGM, whose backbone is synthesized by CSLA2 and decorated by MUCI10, a putative α-1,6-galactosyltransferase (Fig. 3D). The presence of MUCI10 and/or galactosylation is also required for normal glucomannan backbone synthesis since *muci10* mutants had 30-50% lower Glc and Man levels than wild-type (Fig. 2R, Fig 3B). While GGM is primarily decorated with single α-1,6-Gal residues, *muci10-1* mucilage had significant reductions in both t-Gal and 2-Gal linkages (Fig. 3B). One out of every six 2,4-Man units might be substituted with β-1-2-Gal-α-1-6-Gal (Fig. 3D), a disaccharide found in GGM secreted by suspension-cultured tobacco cells (Eda et al., 1985; Sims et al., 1997).

***MUCI10* is Essential for the Distribution of HM in Adherent Mucilage**

To corroborate the biochemical changes detected in *csla2* and *muci10* mucilage extracts, we immunolabeled whole seeds with two monoclonal antibodies. INRA-RU1 binds unbranched RG I chains (Ralet et al., 2010), while LM21 binds effectively to all HM polymers, regardless of their degree of substitution (Marcus et al., 2010). Wild-type and mutant mucilage showed a similar INRA-RU1 labeling (Fig. 4, A to F), consistent with normal pectin synthesis. Mucilage LM21 signals could only be observed with a sensitive hybrid detector (Fig. 4, G and J), likely because GGM represents at most 2.5 % of wild-type mucilage (Table 1). LM21 labeled wild-type mucilage from the basal surface of columellae to the outer edge of the adherent mucilage capsule (Fig. 4G). However, LM21 signals were absent from ray-like regions above the columellae of wild-type (Fig. 4J), and *gt6-1* seeds (Supplemental Fig. S3). Strikingly, no LM21 signals were detected in the mucilage capsules of *csla2-3*, *muci10-2* (Fig. 3), and *muci10-2 gt6-1* (Supplemental Fig. 3). Since these mutants contained 50-80% lower amounts of GGM sugars (Fig. 2R), LM21 epitopes might be reduced below the detection threshold.

GGM Is Required for the Synthesis and Distribution Cellulose in Mucilage

As our *muci10-1* linkage data suggested a 45% decrease in cellulose (*t*-test, $P = 0.065$; Fig. 3A), which can be tightly associated with GGM (Eronen et al., 2011), we examined the structure of cellulose in mucilage using multiple probes and techniques. Pontamine Fast Scarlet 4B (S4B) is a cellulose-specific fluorescent dye (Anderson et al., 2010), and stained ray-like structures in

wild-type mucilage (Fig. 5 and Supplemental Fig. S4; Harpaz-Saad et al., 2011; Mendu et al., 2011; Griffiths et al., 2014). The *csla2-3* and *muci10*-2 mucilage capsules showed decreased S4B fluorescence compared to wild-type, as well as a more compact cellulose distribution (Fig. 5), consistent with RR staining defects (Fig. 2). Surprisingly, these defects appeared to be as severe as in the *cesa5-1* cellulose mutant (Supplemental Fig. S4). Similar to S4B, *muci10-1* and *csla2-3* mucilage showed reduced staining with calcofluor, a β-glycan fluorescent dye (Fig. 6).

Despite decreased S4B and calcofluor staining, the mucilage capsules of GGM mutants were more readily labeled by CBM3a (Fig. 6, Supplemental Fig. S5), a carbohydrate binding module that recognizes crystalline cellulose (Blake et al., 2006; Dagel et al., 2011). CBM3a epitopes were diffuse in wild-type mucilage, but formed cap-like structures that topped *csla2-3* and *muci10-1* calcofluor-stained rays (Fig. 6, F and I). In contrast to the CBM3a labeling, the birefringence of crystalline cellulose in mucilage agreed with the S4B and calcofluor staining. Birefringent rays were equally reduced in three *muci10* alleles and *csla2-3* compared to the wild type (Fig. 7, A to E), but were entirely absent in the *cesa5-1* mutant (Fig. 7F), as previously reported (Sullivan et al., 2011). Consistent with the birefringence results, the seeds of GGM mutants contained intermediate amounts of crystalline cellulose compared to the wild type and *cesa5-1* (Fig. 7I). Therefore, *MUCI10* and *CSLA2* are not only required for the synthesis of GGM in seed coat epidermal cells, but also maintain the structure of cellulose in mucilage.

Cellulose and GGM Are Both Required for Mucilage Attachment to Seeds

Reduced cellulose synthesis in *cesa5* mutants causes severe mucilage detachment from seeds (Harpaz-Saad et al., 2011; Mendu et al., 2011; Sullivan et al., 2011). The *muci10-2* mutant had more non-adherent mucilage than the wild type, but significantly less than *cesa5-1* (Fig. 7J). Polymers containing Man were particularly easy to detach from *muci10-2.* Since *muci10-2* had wild-type levels of total mucilage sugars (Table 1), and only an 8% overall reduction in their adherence, its 25% smaller RR-stained capsule may also result from increased compactness of adherent polysaccharides (Fig. 2Q).

Previously, *csla2-1* mucilage capsules were easily digested by an endo-β-1,4-glucanase from *Aspergillus niger* (Yu et al., 2014). A 90 min treatment with a similar β-glucanase, purified from *Trichoderma longibrachiatum*, fully detached *csla2-3* and *muci10-1* adherent mucilage, but had minor effects on the wild type (Supplemental Fig. S6). The *muci10-1* seeds had clear mucilage detachment after only a 50 min β-glucanase digestion (Fig. 8), showing that cell wall architecture was weakened by the loss of GGM, and that β-Glc linkages maintain mucilage

adherence. While β-Glc linkages are typically derived from cellulose, they also form GGM along with α-Gal and β-Man linkages (Fig. 3D).

To test if GGM itself mediates adherence, we digested mucilage with α-Galactosidase and/or β-Mannanase, two *Aspergillus niger* enzymes that exhibit synergistic degradation of galactomannan (Manzanares et al., 1998). Compared to the buffer control, single enzyme treatments slightly enlarged the mucilage capsules and obscured the RR staining differences between wild-type and *muci10-1* (Fig. 8). Counterstaining revealed that the cellulosic dye S4B could not penetrate RR-stained adherent mucilage capsules (Fig. 9, A to C). Strikingly, wild-type and *muci10-1* seeds digested with both α-Galactosidase and β-Mannanase were surrounded by S4B-stained cellulosic rays (Fig. 9 D to I), but no RR-stained pectin (Fig. 8, M and N). The digested *muci10-1* seeds had reduced S4B fluorescence compared to the wild type (Fig. 9, E and H), similar to *muci10-2* intact mucilage capsules (Fig. 5, Supplemental Fig. S4). The digested seeds also displayed disk-like structures visible with transmitted light and stained by S4B (Fig. 9, D to I), resembling the detached primary cell walls of the *fly1* mutant (Voiniciuc et al., 2013). These results suggest that polymers containing α-Gal and β-Man linkages, namely GGM, are required for the adherence of pectin to Arabidopsis seeds.

MUCI10 Controls Mucilage Density Independently of Calcium Cross-Links

Dextran molecules labeled with fluorescein isothiocyanate (FITC) can be used to examine mucilage porosity (Willats et al., 2001). While 4 kDa and 20 kDa FITC-Dextrans reached the seed surface, 40 kDa molecules were excluded from thin rays in the wild type, and absent from wide mucilage columns in *muci10-1* and *muci10-2* (Supplemental Fig. S7). Accordingly, 70 kDa FITC-Dextrans were largely absent from *muci10* and *csla2-3* mucilage, but only partially excluded from rays in the wild type (Fig. 10, A to D). In *cesa5-1*, which retains cellulosic rays despite reduced adherent mucilage (Supplemental Fig. S4), 70 kDa molecules reached the seed surface (Fig. 10F). Therefore, *muci10* mutants not only had an increase in mucilage detachment but also had a denser mucilage capsule formed by the adherent polysaccharides.

Since the compactness of *csla2-1* was suggested to result from increased calcium cross-links in mucilage (Yu et al., 2014), we investigated how calcium ions affect *muci10* staining defects (Fig. 10, G to L), by treating seeds with $CaCl_2$ and ethylenediaminetetraacetic acid (EDTA), a divalent cation chelator. $CaCl_2$ treatment prevents mucilage extrusion from mutants that can form more HG cross-links (Voiniciuc et al., 2013), but did not impair *muci10* mucilage release (Fig. 10K). EDTA rescues mucilage defects caused by increased calcium cross-links (Rautengarten et al., 2008; Saez-Aguayo et al., 2013; Voiniciuc et al., 2013), but did not expand

the *muci10* mucilage capsule (Fig. 10L) to the wild-type level (Fig. 10I). Since *muci10* mucilage was more compact than wild-type regardless of the presence of calcium, the denser mucilage is most likely the direct result of decreases in GGM, rather than increased HG cross-links.

The *muci10* Mutant Only Shows Major Defects in Seed Mucilage Architecture

To explore if the function of *MUCI10* extends beyond the mucilage of SCE cells, and to elucidate the role of *GT6*, we examined their mutant phenotypes in other cell walls. The dry seed surface morphology of all the mutants examined, including *muci10 gt6*, was similar to the wild type with scanning electron microscopy (SEM; Supplemental Fig. S8). No clear differences in SCE cell shape or size were detected. Since *GT6* may be expressed in sub-epidermal seed coat layers (Supplemental Fig. S1C), we analyzed the distribution of HM epitopes labeled by LM21 in cryo-sections of *muci10-2*, *gt6-1*, and *muci10-2 gt6-1* mature seeds (Supplemental Fig. S9). Similar to the whole mount immunolabeling of adherent mucilage (Fig. 4, and Supplemental Fig. 3), LM21 epitopes surrounded wild-type and *gt6-1* columellae (Supplemental Fig. S9). The analysis of cryo-sectioned seeds did not reveal any clear defects in other cell walls of the seed, suggesting that *MUCI10* specifically affects GGM synthesis in SCE cells. Accordingly, *muci10* and *gt6* single and double mutants were morphologically similar to wild-type plants throughout development. While CSLA2 and related isoforms are required for the synthesis of HM in stems (Goubet et al., 2009), *MUCI10* and *GT6* did not affect the cell wall composition of this tissue (Supplemental Fig. S10), consistent with unbranched glucomannan representing the main HM in Arabidopsis stems (Goubet et al., 2009).

MUCI10-sYFP Proteins Are Sensitive to Brefeldin A and Co-Localize with ST-RFP

MUCI10 tagged with sYFP, a yellow super fluorescent protein (Kremers et al., 2006), localized to small punctae in Arabidopsis cells, while the sYFP tag alone was diffused in the cytosol (Fig. 11, A and B). The small punctae of both MUCI10-sYFP and Wave22Y, a Golgi marker (Geldner et al., 2009), aggregated into large compartments (Fig. 11, C to F), after cells were treated with Brefeldin A (BFA), an inhibitor of secretion (Nebenführ et al., 2002). In addition, MUCI10-sYFP proteins co-localized with the Golgi marker ST-RFP (Teh and Moore, 2007), when stably expressed in Arabidopsis leaf epidermal cells (Fig. 11, G to I). These results are consistent with MUCI10/GTL6 serving as a Golgi marker in multiple proteomic studies (Dunkley et al., 2004; Dunkley et al., 2006; Nikolovski et al., 2012; Nikolovski et al., 2014).

The Degree of Galactosylation Is Critical for GGM Synthesis and Mucilage Properties

We isolated four independent *muci10-1 35S:MUCI10-sYFP* T_1 plants, which displayed small fluorescent punctae (Fig. 11). Analysis of total mucilage extracts from the resulting seeds showed that the MUCI10-sYFP proteins could at least partially complement the reduced GGM sugar content of *muci10-1*, unlike the *35S:sYFP* control (Fig. 12A). While, all four *muci10-1* complemented lines had fully rescued levels of Glc and Man, only line #1 had a degree of galactosylation that was close to the wild-type mucilage. The other three lines had intermediate Gal levels (Fig. 12A), and displayed equally compact mucilage capsules to the *muci10-1* and *muci10-1 35S-sYFP* seeds (Fig. 12J). Interestingly, line #1 had large RR-stained mucilage capsules, similar in size to the wild type (Fig. 12, B to J). This complemented line also resembled the wild type after enzymatic digestion (Fig. 8), and in the 70 kDa FITC-Dextran experiment (Fig. 10). Since line #1 only differed from the other T_1 lines by its high Gal content, the precise degree of GGM substitution may be essential for mucilage properties.

MUCI10 Is Required for the Extensive Decoration of Glucomannan Synthesized by CSLA2

To validate that *MUCI10* functions downstream of *CSLA2* in the synthesis of GGM (Fig. 3D), we isolated a *muci10-1 csla2-3* homozygous double mutant. This double mutant resembled the *csla2-3* single mutant in our analysis of RR staining (Fig. 12E), mucilage area (Fig. 12J), cellulose birefringence (Fig. 7H), and CBM3a labeling (Fig. 6, J to L; Supplemental Fig. S5, J to L). Furthermore, the *35S:MUCI10-sYFP* transgene could not complement *csla2-3* (Fig. 12I), consistent with the *csla2-3* mutation being epistatic to *muci10-1* (Fig. 3D). Although MUCI10 and its paralog likely function as α-1,6-galactosyltransferases, we could not confirm this activity *in vitro.* GST-tagged soluble MUCI10 and GT6 proteins purified from *Escherichia coli* were unable to add Gal to available mannan or glucomannan substrates (Supplemental Fig. S11). Similarly, *Nicotiana benthamiana* microsomes containing full-length MUCI10 proteins tagged with YFP did not show any incorporation of [^{14}C]Gal into mannohexaose relative to controls.

***CSLA2* and *MUCI10* Might Not Be Sufficient for GGM Synthesis**

Via an independent screen, we identified multiple natural accessions with mucilage defects similar to the *muci10* and *csla2* T-DNA mutants. Lm-2 (Le Mans, France), Ri-0 (Richmond, British Columbia, Canada), and Lc-0 (Loch Ness, Scotland, United Kingdom) lacked the HM epitopes recognized by LM21 in Col-0 wild-type mucilage (Supplemental Fig. S3), but had normal dry seed surface morphology (Supplemental Fig. S8). According to the Arabidopsis 1001 Genomes project (http://signal.salk.edu/atg1001/3.0/gebrowser.php; Cao et al., 2011), these

natural accessions do not have unique mutations in the *CSLA2* or *MUCI10* coding regions. This could indicate additional genes required for HM synthesis are mutated in the natural accessions.

DISCUSSION

Although Arabidopsis seed mucilage has been exploited for more than a decade to study cell wall production, only a few enzymes directly required for polysaccharide synthesis in SCE cells have been identified so far (Voiniciuc et al., 2015). To tackle this problem, we conducted a reverse genetic screen for *MUCI* genes that has predicted many glycosyltransferases. Using eight gene baits in multiple co-expression tools, we generated a more comprehensive set of candidate genes for cell wall biosynthesis than previous approaches that used only one or two baits (Vasilevski et al., 2012; Ben-Tov et al., 2015). *MUCI10*, the first of these genes to be characterized in detail, encodes a putative α-1,6-galactosyltransferase related to the fenugreek TfGMGT enzyme that decorates mannan chains with t-Gal residues (Edwards et al., 1999). As suggested by the public microarray data and qRT-PCR analysis (Fig. 1, D and E), *MUCI10* is required for mucilage synthesis during seed coat development. *MUCI10* facilitates the extensive galactosylation of glucomannan in mucilage, a role consistent with a functional paralog of *TfGMGT*. *GT6*, the closest paralog of *MUCI10*, is also expressed in seeds but its transcriptional profile is not consistent with mucilage production (Supplemental Fig. S1). Indeed, *gt6* mutants and a *muci10 gt6* double mutant indicate that *GT6* is not critical for mucilage structure.

MUCI10 Enables the Synthesis of Highly Galactosylated Glucomannan in Mucilage

Mutations in *MUCI10* primarily disrupted HM synthesis in mucilage (Fig. 3A; Fig 4). Our detailed characterization of *muci10* mutants and re-analysis of *csla2-3* revealed that GGM represents at least 80% of Man-containing polymers in Arabidopsis seed mucilage. The initial study of *csla2* mucilage focused exclusively on glucomannan (Yu et al., 2014), and most likely underestimated the abundance of HM in mucilage and its degree of branching. In our linkage analysis (Table 2), wild-type mucilage contained two branched 2,4-Man residues for every unbranched 4-Man unit, consistent with the presence of highly branched GGM rather than unbranched glucomannan. While four independent *muci10* insertion mutants and *csla2-3* displayed equally compact mucilage capsules compared to wild-type seeds (Fig. 2Q), biochemical analysis revealed distinct underlying defects (Fig. 2R). Consistent with CSLA2 synthesizing the backbone of GGM (Fig. 3D), its absence resulted in a significant loss of Gal, Glc and Man residues in mucilage, almost in a 1:1:1 molar ratio (Table 1). In contrast, *muci10*

mutants had a unique biochemical defect, with significantly greater reductions of Gal compared to Glc and Man (Fig. 2R). The *muci10-1* knockout mutant had 81% less t-Gal, a five-fold lower ratio of branched 4,6-Man to unbranched 4-Man (Fig. 3B, Table 2), and a four-fold increase in LM22 epitopes (Fig. 3C) relative to the wild type. Since the LM22 antibody only effectively binds non-galactosylated HM (Marcus et al., 2010), wild-type mucilage contained highly branched HM, while *muci10* mutants had an exceptionally low degree of HM galactosylation.

Our phenotypic analysis of *muci10-1 35S:MUCI10-sYFP* lines indicates that the degree of galactosylation is of paramount importance for the functions of GGM in mucilage (Fig. 12). The addition of some Gal side chains and/or the presence of MUCI10 in a protein complex appear to be essential for the normal synthesis of the GGM backbone by CSLA2, since *muci10* mutants have lower Glc and Man levels (Fig. 2R, Fig 3B). Indeed, all HM polymers are likely synthesized in a highly galactosylated form in the Golgi (Scheller and Ulvskov, 2010). An intermediate Gal level in three independent transformants was sufficient to rescue the GGM backbone sugars to wild-type level, but was not high enough to rescue the compact mucilage defect (Fig. 12). The *muci10 csla2* double mutant supports the model proposed in Fig. 3D, since it resembled the *csla2* single mutant in our analysis of pectin (Fig. 12), and cellulose structure (Fig. 6, Fig. 7). Furthermore, the *35S:MUCI10-sYFP* transgene could not complement the *csla2* mutant (Fig. 12), consistent with *MUCI10* functioning downstream of *CSLA2* in the synthesis of GGM.

MUCI10 **Is Critical for the Organization of Seed Mucilage Polysaccharides**

The loss of highly substituted GGM in *muci10* is associated with smaller mucilage capsules. This phenotype is best explained by the partial detachment of certain polysaccharides, and an increased density of the polymers that remain attached to the seed. Since Man-containing polymers were particularly easy to detach from *muci10* (Fig. 7J), HM with a low degree of galactosylation might be less adherent, and could explain the lack of LM21 epitopes in *muci10* and *csla2* adherent mucilage capsules (Fig. 4). The 8% increased detachment of *muci10* mucilage only partially explains the ~30% smaller capsules. FITC-Dextran experiments indicate molecules above 20 kDa are preferentially excluded from *muci10* and *csla2-3* mucilage capsule, consistent with increased density of the adherent polysaccharides (Supplemental Fig. S7, Fig. 10). Although the denser *csla2* mucilage was proposed to result from increased calcium cross-links (Yu et al., 2014), *muci10* capsules were more compact than wild-type, regardless of the presence or absence of calcium ions (Fig. 10).

Our analysis of single and double mutants shows that GGM synthesized by CSLA2 and MUCI10 maintains the structure of cellulose in seed mucilage. GGM mutants had decreased

calcofluor and S4B staining of cellulose, reduced birefringence and less crystalline cellulose in seeds (Fig. 5, Fig. 6, Fig. 7), but were usually less severe than the *cesa5-1* mutant. CBM3a labelled cap-like structures around *muci10-1* and *csla2-3* single and double mutants seed, as previously reported (Yu et al., 2014). As discussed in a recent review (Voiniciuc et al., 2015), CBM3a specificity and/or accessibility is puzzling. The *cesa5* (this study; Sullivan et al., 2011), *csla2* (this study; Yu et al., 2014), and *muci10* (this study) mucilage had increased CBM3a labeling, despite clear decreases in cellulose content via other probes and techniques.

GGM Scaffolds and Cellulosic Rays Maintain the Architecture of Mucilage

Two distinct structures, which partially overlap, are likely to control mucilage architecture. SCE cells release cellulosic rays that extend above columellae and anchor mucilage polymers to the seed (Fig. 5 and Supplemental Fig. S4; Harpaz-Saad et al., 2011; Mendu et al., 2011; Sullivan et al., 2011; Griffiths et al., 2014; Griffiths et al., 2015). We propose that a GGM scaffold surrounds the cellulosic rays in the mucilage capsule (Fig. 4J), and controls the spacing of mucilage polymers. GGM can form tight associations with cellulose (Eronen et al., 2011), while its Gal side chains can generate “hairy” regions that promote gelation (Dea et al., 1977). While the cellulosic ray is indispensable for adherence, highly branched GGM scaffolds primarily control mucilage density. Reduced galactosylation may cause the GGM scaffolds to flatten and the surrounding polymers to either detach from the seed, or to be more tightly packed in the adherent mucilage capsule.

Consistent with this model, *muci10* and *csla2* had compromised mucilage architecture and were more susceptible to β-glucanase digestion than the wild type (Fig. 8, Supplemental Fig. S6). β-Glc linkages, primarily from cellulose, are essential for the adherence of mucilage polysaccharides. Using *Aspergillus niger* α-Galactosidase and β-Mannanase, which synergistically degrade galactomannan (Manzanares et al., 1998), we demonstrated that polymers containing α-Gal and β-Man linkages, mainly GGM, are also required for the adherence of pectin, but not cellulose, to the seed (Fig. 8, Fig. 9). This further supports the role of GGM as a scaffold that maintains the distribution of pectic polysaccharides.

MUCI10 Is Essential, but Not Sufficient for GGM Synthesis

CSLA2 and MUCI10 are Golgi-localized proteins (Fig. 11, Nikolovski et al., 2014; Yu et al., 2014), and are likely the key enzymes required for GGM synthesis in the Golgi apparatus. Although we did not detect *in vitro* galactosyltransferase activity for MUCI10 recombinant proteins purified from *E. coli* or expressed in *N. benthamiana* microsomes, only a few plant

glycosyltransferases have been biochemically characterized through direct assays. Such enzymes are typically highly unstable membrane-bound proteins (Brown et al., 2012). However, MUCI10-sYFP could fully complement the biochemical defects and altered properties of the *muci10-1* mutant. Consistent with MUCI10 substituting glucomannan synthesized by CSLA2, the MUCI10-sYFP protein could not rescue the *csla2* mucilage defects.

The lack of MUCI10 *in vitro* activity may indicate that GGM synthesis requires a protein complex. The synthesis of xyloglucan, another hemicellulose, requires homo- and hetero-complexes of CSLC4, a β-1-4-glucan synthase (Cocuron et al., 2007), and XXT proteins (Chou et al., 2012; Chou et al., 2014). Since CSLA2 and MUCI10 are members of the same CAZy GT families as CSLC4 and XXT, respectively, future studies should investigate if similar protein-protein interactions facilitate GGM synthesis. Indeed, two proteins (MSR1 and MSR2) were already proposed to promote glucomannan synthesis by stabilizing CSLA enzymes (Wang et al., 2012b). An alternative possibility is that MUCI10 requires glucomannan acceptors, in contrast to the fenugreek TfGMGT enzyme that uses pure manno-oligosaccharides with a length of at least five units (Edwards et al., 1999). This could not be fully tested due to the limited availability of glucomannan acceptor substrates. Although purified GST-MUCI10 proteins were not active on glucomannan disaccharides and trisaccharides (Supplemental Fig. S8), these substrates may be too short to function as acceptors.

Our detailed characterization of the role of *MUCI10* in SCE cells significantly expands our knowledge of polysaccharide biosynthesis and demonstrates that wild-type Arabidopsis mucilage contains highly substituted GGM rather than unbranched glucomannan. This study highlights that, despite primarily consisting of pectin, Arabidopsis seed mucilage is a valuable model to study hemicellulose synthesis. We show that MUCI10 is responsible for GGM branching, which influences the distribution of pectin polymers and the structure of cellulose. Since GGM is the most abundant hemicellulose in the secondary walls of gymnosperms, understanding the biosynthesis of this polymer may facilitate improvements in the production of valuable commodities from softwoods. Further investigation of Arabidopsis natural variants with defects similar to *muci10* may allow us to identify additional genes involved in HM synthesis.

MATERIALS AND METHODS

Plant Material

Mutants (*muci10-1*, SALK_061576; *muci10-2*, SALK_002556; *muci10-3*, SALK_133170; *muci10-4*, SALK_033930; *gt6-1*, SALK_134982; *gt6-2*, SALK_151067) were selected from the SALK collection (Alonso et al., 2003; http://signal.salk.edu/cgi-bin/tdnaexpress). The *cesa5-1*

(SALK_118491; Mendu et al., 2011; Griffiths et al., 2014) and *csla2-3* (SALK_149092; Yu et al., 2014) mutants were previously described. The T-DNA lines, Wave22Y (N781656) and ST-RFP (N799376) seeds were ordered from the Nottingham Arabidopsis Stock Centre (http://arabidopsis.info). The Lm-2 (31AV), Ri-0 (160AV), and Lc-2 (171AV) accessions were obtained from the Versailles Arabidopsis Stock Center (http://publiclines.versailles.inra.fr). The plants were grown as previously described (Voiniciuc et al., 2015), in individual 7x7x8 cm pots, under constant light (around 170 μE m^{-2} s^{-1}), temperature (20°C) and relative humidity (60%). Only the seeds analyzed in Supplemental Tables S2 and S3 were produced in a chamber with a 12/12 h photoperiod. Flowering plants were covered with ARACON tubes (Betatech bvba, http://www.arasystem.com), to prevent cross fertilization of flowers and seed dispersal. Seeds were harvested by shaking mature plants into individual brown paper bags.

Genotyping, RNA Isolation and RT-PCR Analysis

The genotyping, RT-PCR and cloning primers used are listed in Supplemental Table S4. PCR genotyping was performed using the Touch-and-Go method (Berendzen et al., 2005).

For RNA isolation, silique developmental stages were established along the stem length by dissecting seeds and analyzing the embryo stage. Counting the first open flower as one, siliques 13+14 (heart stage), 20+21 (linear cotyledon), and 26+27 (mature green)were harvested for each genotype. Seed coat microarray data indicates that the heart stage and linear cotyledon stages are equivalent to 3 and 7 DPA, respectively (Dean et al., 2011; Belmonte et al., 2013). Whole siliques were immediately placed on dry ice and stored at –80°C. RNA was isolated using the ZR Plant RNA MiniPrep kit (Zymo Research, Cat# R2024), according to the manufacturer's instructions, and included on-column DNase I (Zymo Research, Cat# E1009) digestion to remove any DNA contaminants. RNA was quantified using a NanoDrop 1000 (Thermo Fisher Scientific), and 200 ng was used as template for the iScript cDNA Synthesis Kit (Bio-Rad, Cat# 170-8891). Primers for RT-PCR amplification were designed using the QuantPrime (http://www.quantprime.de) tool (Arvidsson et al., 2008). RT-PCR fragments were amplified for 33 cycles with Red-Taq DNA-Polymerase (VWR International, Cat# 733-2546P). *GAPC1* was used as a reference gene (Dean et al., 2007), and DNA was stained with GelRed (Biotium).*UBQ5* served as a reference gene for qRT-PCR (Gutierrez et al., 2008). Amplification efficiencies were determined using a serial dilution of DNA, and the Pfaffl method was used to calculate fold changes in gene expression relative to the wild-type heart stage (Pfaffl, 2001; Fraga et al., 2008).

Ruthenium Red (RR) Staining

Staining was carried out using cell culture plates with 24 wells (VWR International GmbH, Cat# 734-2325). Around 30 seeds were added to a well pre-filled with 500 µL of water, and imbibed for 5 min with gentle mixing. After removing the water, seeds were stained with 300 µL of 0.01% (w/v) ruthenium red (VWR International GmbH, Cat# A3488.0001) for 5 min. The dye was replaced with 300 µL of water, and each well was imaged with a Leica MZ12 stereomicroscope equipped with a Leica DFC 295 camera. All images were analyzed and processed using Fiji (http://fiji.sc/Fiji; Schindelin et al., 2012).

Enzymatic digestion of mucilage capsules was also performed in a 24-well plate format. Dry seeds were imbibed in 500 µL of 0.1 M sodium acetate buffer pH 4.5, with or without 10 units of the following enzymes (all from Megazyme): *Trichoderma longibrachiatum endo*-1,4-β-D-glucanase (Cat# E-CELTR), *Aspergillus niger* α-galactosidase (Cat# E-AGLAN), and/or *Aspergillus niger* endo-1,4 β -Mannanase (Cat# E-BMANN). Plates were incubated for 50 to 90 min (as specified in the figures) at 125 rpm and 37-40°C. The buffer was then removed, and each well was rinsed once with 500 µL of water, prior to RR staining.

The effect of calcium cross-links on mucilage dimensions was investigated by hydrating seeds in 500 µL of water, 50 mM $CaCl_2$ or 50 mM EDTA pH 9.5 for 60 min at 125 rpm in a 24-well plate. Seeds were rinsed twice with water, and then stained with RR.

Quantification of Mucilage Area

Image analysis followed ImageJ instructions (http://rsb.info.nih.gov/ij/docs/menus/analyze.html). Regions of interest were segmented in Fiji using distinct RGB Colour Thresholding (min-max) parameters: Mucilage+Seed (Red 0-255; Green 0-115; Blue 0-255), Seed (Red 0-120; Green 0-255; Blue 0-255). Areas of the two regions of interest were measured using the Analyze Particles function (circularity = 0.5 - 1.0), excluding edges and extreme particle sizes, and were subtracted in Excel to calculate the dimensions of only the RR-stained mucilage capsules.

Statistical Analyses

The dimensions of mucilage capsules, and their biochemical composition (see detailed methods below) were normally distributed according the Shapiro-Wilk test (Shapiro and Wilk, 1965), performed using the Real Statistics Resource Pack (http://www.real-statistics.com) for Microsoft Excel 2010. Statistically significant changes were identified through the T.TEST function in Microsoft Excel 2010, using two-tailed distribution and assuming equal variance of two samples.

The significant changes presented in Supplemental Fig. S1 were identified using data obtained from the Bio-Analytic Resource (Winter et al., 2007; http://bar.utoronto.ca), and the unpaired *t*-test on the GraphPad website (http://www.graphpad.com/quickcalcs/ttest1/?Format=SD).

Total Mucilage Extraction and Monosaccharide Composition

Around 5 mg seeds were precisely weighed in 2 mL Safe-Lock Eppendorf tubes. A serial dilution of a nine-sugar mixture (fucose, rhamnose, arabinose, galactose, glucose, xylose, mannose, galacturonic acid, glucuronic acid; all obtained from Sigma-Aldrich) was performed in 2 mL screw-cap tubes. One mL of water, containing 30 µg ribose as an internal standard, was added to all the samples and standards. Total mucilage was extracted by vigorously shaking the seed-containing tubes for 15 min at 30 Hz in a Retsch MM400 ball mill using two 24 TissueLyser Adapters (Qiagen, Hilden, Germany). The adapters were then rotated 180 degrees and mixed for an additional 15 min at 30 Hz. The seeds were allowed to settle at the bottom of each tube, and 800 µL of the supernatant was transferred to a screw-cap tube. Samples and standards were dried under pressurized air at 45°C using a Techne Dri-Block DB 3D heater. Once dry, 300 µL of 2 N trifluoroacetic acid (TFA) was added to each tube. Tubes were capped tightly, vortexed, and heated for 90 min at 121°C. The heating blocks and the samples were then cooled on ice. After brief centrifugation, tubes were uncapped and the TFA was evaporated under pressurized air at 45 °C. Dried samples and standards were then re-suspended in 400 µL of water. Monosaccharides were quantified by High-Performance Anion-Exchange Chromatography with Pulsed Amperometric Detection (HPAEC-PAD), using a Dionex system equipped with a CarboPac PA20 column and GP50, ED50, and AS50 modules. The column was operated at a constant flow rate of 0.4 mL/min and was equilibrated with 2 mM NaOH for 10 min before sample injection. Neutral sugars were separated with 2 mM NaOH over the course of 18 min. Afterwards, 513 mM NaOH was used for 7.5 min to separate uronic acids. Finally, the column was rinsed with 733 mM NaOH for 4 min. Monosaccharide amounts were normalized to the internal standard and quantified using standard calibration curves.

Quantification of Mucilage Detachment

Non-adherent and adherent mucilage fractions were sequentially extracted from 5 mg seeds in 2 mL Safe-Lock Eppendorf tubes. Non-adherent mucilage was detached by mixing seeds in 1 mL of water for 15 min at 125 rpm using an orbital shaker, with 30 µg ribose as an internal standard. Afterwards, 800 µL of supernatants were transferred to 2 mL screw-cap tubes, dried and prepared for HPAEC-PAD analysis similar to the total mucilage extracts.

After rinsing the seeds twice with water, the adherent mucilage was removed by essentially performing a total mucilage extraction, except that 2-deoxy-D-glucose was used as an internal standard instead of ribose. The supernatants were transferred to 2 mL screw-cap tubes, dried and prepared for HPAEC-PAD analysis similar to the total mucilage extracts. Accordingly, the nine-sugar mixture dilutions were prepared using with 2-deoxy-D-glucose as internal standard.

Glycosyl Linkage Analysis of Total Mucilage Extracts

Total mucilage was extracted from 60 mg seeds using the ball mill method described above. To obtain complete extraction, seeds were split into three 2 mL Safe-Lock Eppendorf tubes with 1 mL of water in each. Supernatants (800 µL) of the extractions were pooled and 400 µL of the pooled sample was used for HPAEC-PAD monosaccharide analysis. The remaining sample was acidified by adding 800 µL of 0.1 M sodium acetate buffer, pH 4.6. The reduction of the uronic acids to their respective 6,6-dideuterio derivatives was carried out as described by (Gibeaut and Carpita, 1991; Huang et al., 2011). For reduction, 0.1 mg 1-cyclohexyl-3-(2-morpholinyl-4-ethyl) carbodiimide (methyl-p-toluene sulfonate) was added to the samples. After 2 h incubation, 0.1 mg sodium borodeuteride together with 1 mL of cold 2 M imidazole, pH 7.0, was added and the sample was incubated on ice for another hour. To remove residual sodium borodeuteride, glacial acid was added drop-wise. After reduction of uronic acids the samples were extensively dialyzed against water followed by lyophilization, the dry samples were solubilized in 200 µL of anhydrous DMSO. Methylation was essentially performed as described by (Gille et al., 2009). For the reaction, an alkaline DMSO solution was prepared using 100 µL of 50 % (w/w) sodium hydroxide that was washed and sonicated several times with anhydrous DMSO (5 mL) and finally suspended in 2 mL of anhydrous DMSO. The alkaline DMSO suspension (200 µL), together with methyl iodide (100 µL), was added to samples. After 3 h incubation, 2 mL of water was added to quench the reaction. Methylated polysaccharides were extracted with 2 mL of dichloromethane, hydrolyzed and derivatized to the corresponding alditol acetates and analyzed by GC-MS as described by (Foster et al., 2010), using sodium borodeuteride for the reduction. Polysaccharide composition was calculated based on linkage analysis using a published protocol (Pettolino et al., 2012).

Monosaccharide Composition of Stem AIR

The bottom 3 cm of the main inflorescence stem from four-week old Arabidopsis plants were harvested and immediately lyophilized. Dry stems were ground for 10 min at 30 Hz using a ball mill and steel balls. Afterwards, 1 mL of 70% (v/v) aqueous ethanol was added and the material

was ground for an additional 10 min at 30 Hz. The insoluble residue was extracted once with 1:1 (v/v) chloroform:methanol and dried under a stream of air. HPAEC-PAD monosaccharide analysis of 2 mg of AIR was performed similar to the total mucilage extracts, except that samples were shaken vigorously in 2 N TFA for 10 min at 20 Hz using a ball mill to fully disperse the AIR pellets prior to hydrolysis.

Crystalline Cellulose Observation and Content Determination

Seeds were hydrated in water for 10 min, and examined on a glass slide with polarized light using a Zeiss Axioplan2 microscope equipped with a Zeiss AxioCam ICc 5 camera. For crystalline content determination, 5 mg of seeds were milled using steel balls for 90 sec at 30 Hz. Alcohol-insoluble residue (AIR) was isolated by two sequential washes with 1 mL of 70% (v/v) ethanol, and centrifugation for 3 min at 20000 *g*. After washing the AIR with 1:1 (v/v) chloroform:methanol, followed by acetone, the pellet was dried for 5 min at 60°C. Crystalline cellulose content was then determined as previously described (Foster et al., 2010), with minor modifications. The 2 mg of dry AIR was mixed with 1 mL of Updegraff reagent at 30 Hz for 90 sec (Updegraff, 1969), before incubation at 100°C for 30 min. After hydrolysis, the Updegraff-resistant pellet (containing only crystalline cellulose) was rinsed once with water, once with acetone, dried, and then hydrolyzed using 200 µL of 72% (v/v) sulfuric acid. The amount of glucose released was quantified using anthrone in a 96-well plate (Foster et al., 2010).

LM22 ELISA Analysis of Non-Galactosylated HM in Mucilage

The ELISA analysis was performed as described (Pattathil et al., 2010), with minor modifications. We used bovine serum albumin (BSA) instead of dry milk, and a ready-to-use 3,3',5,5'-Tetramethylbenzidine (TMB) substrate solution (Sigma-Aldrich, Cat# T4444-100ML). The 50 µL TMB reaction was stopped by adding 50 µL of 1N sulfuric acid (instead of 0.5N). All pipetting and wash steps were manually performed. Total mucilage was extracted from 10 mg of seeds using 1 mL water, and 200 µL aliquots of the supernatant were transferred to a 96-well plate (Corning, Cat# 3598). Based on our monosaccharide data, these aliquots yield 0.4 µg of mannose, which should be sufficient to saturate the wells with HM antigens. The LM22 antibody (PlantProbes, http://www.plantprobes.net) only effectively binds unbranched HM (Marcus et al., 2010).

Immunolabeling Experiments

Whole seeds were immunolabeled as previously described (Macquet et al., 2007), using LM21 (PlantProbes) and INRA-RU1 (INRA, Nantes, France) primary antibodies (Marcus et al., 2010; Ralet et al., 2010). Alexa Fluor 488 (Molecular Probes, Life Technologies) was used as a secondary antibody. Observations were carried out on a Leica SP5 confocal microscope with settings fixed for the detection of the same label in different samples. LM21 labeling was analyzed with a Leica HyD detector (488 nm excitation, 500-550 nm emission). Images were processed identically in Fiji.

For crystalline cellulose labeling, seeds were first shaken in water. Unless otherwise stated, all incubations were performed for 60 min at 200 rpm using an orbital shaker. Seeds were rinsed twice with water, and mixed with 800 µL of phosphate-buffered saline (PBS) for 30 min. The buffer was removed, and mucilage was blocked with 100 µL of 5% (w/v) bovine serum albumin (BSA) in PBS. Seeds were sequentially incubated with 50 µL of His-tagged CBM3a (PlantProbes), anti-His mouse antibody (Sigma-Aldrich, Cat# SAB4600048), and Alexa Fluor 488 goat-anti-mouse. The primary antibody was diluted 1:10, while the secondary antibodies were diluted 1:1000 using 1% (w/v) BSA in PBS solution. Five PBS washes were performed after each of the three incubations. Seeds were counter-stained for 20 min with 2.5 % (w/v) calcofluor white (Sigma-Aldrich, Cat# F3543), rinsed four times with water, and stored overnight in PBS at 4°C. Images were acquired on a Leica SP8 confocal microscope using the following settings: calcofluor (405 nm excitation, 405-452 nm emission), CBM3a signal (488 nm excitation, 491-570 nm emission).

For cryo-sectioning, dry seeds were mounted in a mold (Dutscher, Cat# 040664), which was then completely filled with embedding medium (MM France, NEG50: F/161426), and frozen in liquid nitrogen. Thick (16-20 µm) sections were cut using a CryoStart NX70 (Thermo Scientific) at -20°C, and were transferred onto a PolyLysine slide (Menzel Glaser, Thermo Scientific). For immunolabeling, frozen sections were first treated with 4% (w/v) formaldehyde in PBS for 15 min, then washed three times with PBS (5 min per wash). After blocking with 1% (w/v) milk protein in PBS for 60 min, sections were labeled with LM21 diluted 1/10 with 1% (w/v) milk protein in PBS for 120 min. After three PBS washes, sections were labeled with a goat anti-rat Alexa Fluor 488 (Molecular Probes, Life Technologies) secondary antibody diluted 1/100 with 1% (w/v) milk protein in PBS. Sections were washed three times with PBS, and stained with either 0.1 mg/mL propidium iodide or 0.5% (w/v) calcofluor white. After a final set of washes, sections were examined with a Leica SP5 or a Zeiss LSM 710 confocal microscope: calcofluor

(405 nm excitation, 415-470 nm emission) and Alexa Fluor 488 (488 nm excitation, 500-550 nm emission).

Other Histological Techniques

Surface morphology of dry seeds, mounted onto a Peltier cooling stage with adhesive discs (Deben), was observed with a Hirox SH-1500 tabletop SEM.

Cellulose was stained with 0.01% (w/v) S4B (now sold as Direct Red 23; Sigma-Aldrich, Cat# 212490-50G) in 50 mM NaCl (Anderson et al., 2010; Mendu et al., 2011), and was imaged with Leica SP5 confocal system (561 nm excitation, 570-660 nm emission). Supplemental Fig. S4 images were acquired using a Leica SP8 confocal system (552 nm excitation, 600-650 nm emission).

For Fig. 9, RR-stained seeds were rinsed with water and counter-stained with 200 µL of 0.025% (w/v) S4B in 50 mM NaCl, for 60 min at 125 rpm. After three water washes, seeds were imaged using a Leica SP8 confocal system (552 nm excitation, 600-650 nm emission).

For FITC-Dextran staining in Supplemental Fig. S4, seeds were imbibed in 1 mL of water in 2 mL Eppendorf tubes, and rotated for 60 min at room temperature. The water was then replaced with 1 mL of 0.1M citric acid, 0.2M disodium phosphate (CP) pH 5.0 and mixed for an additional 60 min. Seeds were transferred onto an 8-well sticky slide (Ibidi, Cat# 80828), and mixed with 250 µL CP containing 250 µg FITC-Dextran (TdB Consultancy AB) for 60 min in the dark. FITC (488 nm excitation, 502-542 nm emission) was detected with a Leica SP5 confocal system.

For Fig. 10, seeds were hydrated in 300 µL of 100 mM sodium acetate pH 4.5 for 10 min, and then stained with 300 µL of 1 mg/mL FITC-Dextran 70 kDa (Sigma-Aldrich, Cat# 46945) for 30 min at 125 rpm in a 24-well plate. Seeds were transferred to glass slides and imaged with a Leica SP8 confocal system (488 nm excitation, 502-542 nm emission).

Expression and Analysis of MUCI10-sYFP Subcellular Localization

The *35S:MUCI10-sYFP* construct was generated using the ligation independent cloning (LIC) technique (De Rybel et al., 2011). For cloning, DNA was amplified with Phusion High-Fidelity DNA Polymerase (New England Biolabs). LIC-compatible pPLV vectors were obtained from the Nottingham Arabidopsis Stock Centre. We first amplified the sYFP (720 bp) tag from the pPLV16 vector and inserted it into the BamHI site on the 3' side of the LIC site in the pPLV25 vector (containing the 35S promoter but no fluorescent tag). The new *35S:LIC-sYFP* vector, named pCV01, was verified by Sanger sequencing. We redesigned the reverse LIC adapter primer to allow in-frame fusions to sYFP.

Arabidopsis wild-type genomic DNA was isolated using a commercial kit (GeneON, Cat# PT050). A *MUCI10* fragment (1832 bp) was amplified from the ATG codon until, but excluding the stop codon. The adapter primers required five three-step amplification cycles with a low annealing temperature (55°C), followed by 30 cycles of two-step Phusion PCR with an annealing/extension temperature of 72°C. The *MUCI10* amplicon was gel-purified, and the rest of the LIC procedure was performed as described (De Rybel et al., 2011). The final plasmid was verified by Sanger sequencing, and transformed into *Agrobacterium tumefaciens* GV3101::pMP90::pSOUP cells. Arabidopsis plants were then transformed using a modified floral spray method (Weigel and Glazebrook, 2006), with an infiltration medium containing 5% (w/v) sucrose and 0.02% (v/v) Silwet L-77. Basta-resistant T_1 seedlings were selected on soil using a 10 mg/L glufosinate-ammonium (Sigma-Aldrich, Cat# 45520-100MG) spray. Fluorescence was examined in Arabidopsis seedlings using a Leica SP8 confocal microscope: sYFP (488 nm excitation, 505-550 emission), intrinsic plant fluorescence (488 nm excitation, 615-705 nm emission), and RFP (552 nm excitation, 590-635 nm emission). To avoid crosstalk for co-localization analysis, sYFP and RFP signals were sequentially acquired each line scan.

Cloning of GST protein fusions

The topology of MUCI10 and GT6 proteins was assessed using ARAMEMNON (Schwacke et al., 2003). Truncated *MUCI10* (1188 bp) and *GT6* (1176 bp) sequences (lacking the 5' region encoding an N-terminal transmembrane domain) were amplified from cDNA and were inserted between the *Not*I and *Sal*I sites in the pGEX-5x-3 vector (GE Healthcare). This generated N-terminal fusions to glutathione S-transferase (GST). Plasmids were propagated in NEB 5-alpha *E. coli* (New England Biolabs GmbH), and, after sequence verification, were transformed in BL21(DE3) *E. coli* (New England Biolabs GmbH) cells for protein expression.

GST Fusion Protein Expression and Purification

Protein expression and purification was performed in accordance with the pGEX guide (GE Healthcare). A 3 mL pre-culture of 2x YTA media, containing ampicillin, was inoculated with BL21(DE3) *E. coli* containing the desired plasmid and was incubated overnight at 37°C. The next day, the pre-culture was added to 100 mL of 2x YTA media, containing ampicillin, and was incubated for 3 h until the OD_{600} equaled 0.6. Protein expression was induced using 1 mM isopropyl β-D-1-thiogalactopyranoside (IPTG; Carl Roth, Cat# 2316.2), for 16 h at 20°C. Cell pellets, collected using 7100*g* at 4°C, were suspended in 2500 µL of cold PBS buffer and disrupted on ice for 60-90 sec using a Vibracell 75186 sonicator (pulse method, 50% intensity).

Samples were then mixed with 62.5 µL bacterial protease inhibitor (Carl Roth, Cat# 3758.1), and 125 µL of 20% Triton X-100 on ice for 60 min. The lysate was cleared by spinning at 7100*g* for 10 min 4°C. For affinity purification, 2 mL 50% (v/v) glutathione agarose slurry (Thermo Fisher Scientific Pierce) was added to gravity-flow columns, and rinsed with 10 mL of 50 mM Tris-HCl, 150 mM NaCl, pH 8.0 equilibration buffer (EB). Lysate, mixed with an equal volume of EB, was added to the column. After rinsing with 10 mL of EB, GST-tagged proteins were eluted using 50 mM Tris-HCl, 150 mM NaCl, 10 mM reduced glutathione, pH 8.0. Purified proteins were quantified using the Qubit Protein Assay (Life Technologies).

UDP-Glo Assay for Galactosyltransferase Activity

Activity of GST-tagged proteins was quantified using the UDP-Glo Glycosyltransferase Assay (Promega, Custom Assay CS1681A05) according to the manufacturer's instructions and the GT reaction conditions that were successful for the IRX10-L xylan xylosyltransferase (Urbanowicz et al., 2014). GT reactions (25 µL) containing 50 mM HEPES-NaOH buffer (pH 7.0) and 1.25 µg purified protein was carried out using 800 µM ultra-pure UDP-Gal (Promega, Cat#V7171) as donor and 1 mM of an acceptor substrate. The acceptor substrates (all from Megazyme International Ireland) were: mannotriose (O-MTR), mannotetraose (O-MTE), mannopentaose, (O-MPE), mannohexaose (O-MHE), cellohexaose (O-CHE), glucomannan disaccharides (O-GMMBI) and trisaccharides (O-GMMTR). Cellohexaose, which XXTs bind to (Vuttipongchaikij et al., 2012), was included as a negative control. The galactosyltransferase reactions were incubated for 60 min at 23°C in a 96-well, half-area, white plate (VWR International, Cat# 392-0056). For UDP detection, 25 µL of UDP-Glo detection reagent was added to each reaction and was incubated for 60 min at 23°C. The luminescence of each well was then measured using a Synergy H1M Hybrid Reader (BioTek). A serial dilution of UDP standards (Promega) showed a linear response from 0.01 µM to 12 µM.

***N. benthamiana* Microsome Preparation and Galactosyltransferase Assay**

For transient expression in *N. benthamiana*, we created a *35S:MUCI10-YFP* construct by introducing the pDONR *MUCI10* clone obtained from the JBEI GT collection (Lao et al., 2014) into the pEarleyGate101 vector (Earley et al., 2006), using the LR Clonase II reaction according to the Life Technologies protocol. Constructs were verified by sequencing.

A. tumefaciens GV3101::pMP90 cells carrying the YFP fusion construct or the p19 gene from tomato bushy stunt virus were grown overnight, pelleted at 4000*g* (10 min, 15°C), washed and re-suspended in 10 mM MES, 10 mM $MgCl_2$, 100 µM acetosyringone infiltration buffer, yielding

a final OD_{600} value of 0.15. Leaves of three to four-week old *N. benthamiana* plants grown in a day/night cycle (16/8 h light/dark, 25/24°C, 60% relative humidity) were co-infiltrated with the two *A. tumefaciens* mixtures using a 1 mL syringe. After two additional days of plant growth, protein expression was verified by monitoring YFP fluorescence with an epifluorescence microscope. Three days after infiltration, five entire leaves were harvested and microsomes were extracted (Rennie et al., 2012). Galactosyltransferase activity was determined essentially as previously described (Liwanag et al., 2012), using 40 µg microsomal protein, 10 nCi UDP-[^{14}C]Gal, and 20 mM mannohexaose per 50 µL reaction.

ACKNOWLEDGEMENTS:

The *cesa5-1* seeds were a gift from Krešimir Šola and Dr. George Haughn (UBC, Canada).

AUTHOR CONTRIBUTIONS:

C.V., B.U. and M.G. designed research. C.V. wrote the article, and B.U. and M.G. revised it. M.S. performed cloning and *E.coli* work. A.B. and H.M.N. designed and performed histological analysis. B.Y. performed CBM3a labeling and Updegraff assay. B.E. and H.V.S. designed and performed *N. benthamiana* work. C.V. and M.G. performed remaining experiments. All authors discussed the results, and approved the final manuscript.

LITERATURE CITED

Alonso JM, Stepanova AN, Leisse TJ, Kim CJ, Chen H, Shinn P, Stevenson DK, Zimmerman J, Barajas P, Cheuk R, et al (2003) Genome-wide insertional mutagenesis of Arabidopsis thaliana. Science **301**: 653–657

Anderson CT, Carroll A, Akhmetova L, Somerville C (2010) Real-time imaging of cellulose reorientation during cell wall expansion in Arabidopsis roots. Plant Physiol **152**: 787–96

Arvidsson S, Kwasniewski M, Riaño-Pachón DM, Mueller-Roeber B (2008) QuantPrime--a flexible tool for reliable high-throughput primer design for quantitative PCR. BMC Bioinformatics **9**: 465

Belmonte MF, Kirkbride RC, Stone SL, Pelletier JM, Bui AQ, Yeung EC, Hashimoto M, Fei J, Harada CM, Munoz MD, et al (2013) Comprehensive developmental profiles of gene activity in regions and subregions of the Arabidopsis seed. Proc Natl Acad Sci U S A **110**: E435–44

Benová-Kákosová A, Digonnet C, Goubet F, Ranocha P, Jauneau A, Pesquet E, Barbier O, Zhang Z, Capek P, Dupree P, et al (2006) Galactoglucomannans increase cell population density and alter the protoxylem/metaxylem tracheary element ratio in xylogenic cultures of Zinnia. Plant Physiol **142**: 696–709

Ben-Tov D, Abraham Y, Stav S, Thompson K, Loraine A, Elbaum R, De Souza A, Pauly M, Kieber JJ, Harpaz-Saad S (2015) COBRA-LIKE 2, a member of the GPI-anchored COBRA-LIKE family, plays a role in cellulose deposition in Arabidopsis seed coat mucilage secretory cells. Plant Physiol **167**: 711–24

Berendzen K, Searle I, Ravenscroft D, Koncz C, Batschauer A, Coupland G, Somssich IE, Ulker B (2005) A rapid and versatile combined DNA/RNA extraction protocol and its application to the analysis of a novel DNA marker set polymorphic between Arabidopsis thaliana ecotypes Col-0 and Landsberg erecta. Plant Methods **1**: 4

Bernal AAJ, Yoo CC-M, Mutwil M, Jensen JKJ, Hou G, Blaukopf C, Sørensen I, Blancaflor EB, Scheller HV, Willats WGT (2008) Functional analysis of the cellulose synthase-like genes CSLD1, CSLD2, and CSLD4 in tip-growing Arabidopsis cells. Plant Physiol **148**: 1238–53

Blake AW, McCartney L, Flint JE, Bolam DN, Boraston AB, Gilbert HJ, Knox JP (2006) Understanding the biological rationale for the diversity of cellulose-directed carbohydrate-binding modules in prokaryotic enzymes. J Biol Chem **281**: 29321–9

Brown C, Leijon F, Bulone V (2012) Radiometric and spectrophotometric in vitro assays of glycosyltransferases involved in plant cell wall carbohydrate biosynthesis. Nat Protoc **7**: 1634–50

Burton RA, Fincher GB (2012) Current challenges in cell wall biology in the cereals and grasses. Front Plant Sci **3**: 130

Burton RA, Gidley MJ, Fincher GB (2010) Heterogeneity in the chemistry, structure and function of plant cell walls. Nat Chem Biol **6**: 724–32

Caffall KH, Pattathil S, Phillips SE, Hahn MG, Mohnen D (2009) Arabidopsis thaliana T-DNA mutants implicate GAUT genes in the biosynthesis of pectin and xylan in cell walls and seed testa. Mol Plant **2**: 1000–14

Cao J, Schneeberger K, Ossowski S, Günther T, Bender S, Fitz J, Koenig D, Lanz C, Stegle O, Lippert C, et al (2011) Whole-genome sequencing of multiple Arabidopsis thaliana populations. Nat Genet **43**: 956–63

Carpita N, Tierney M, Campbell M (2001) Molecular biology of the plant cell wall: Searching for the genes that define structure, architecture and dynamics. Plant Mol Biol **47**: 1–5

Cavalier DM, Lerouxel O, Neumetzler L, Yamauchi K, Reinecke A, Freshour G, Zabotina OA, Hahn MG, Burgert I, Pauly M, et al (2008) Disrupting two Arabidopsis thaliana xylosyltransferase genes results in plants deficient in xyloglucan, a major primary cell wall component. Plant Cell **20**: 1519–37

Chou Y-H, Pogorelko G, Young ZT, Zabotina OA (2014) Protein-Protein Interactions Among Xyloglucan-Synthesizing Enzymes and Formation of Golgi-Localized Multiprotein Complexes. Plant Cell Physiol **56**: 255–267

Chou Y-H, Pogorelko G, Zabotina OA (2012) Xyloglucan Xylosyltransferases XXT1, XXT2, and XXT5 and the Glucan Synthase CSLC4 Form Golgi-Localized Multiprotein Complexes. PLANT Physiol **159**: 1355–1366

Cocuron J-C, Lerouxel O, Drakakaki G, Alonso AP, Liepman AH, Keegstra K, Raikhel N, Wilkerson CG (2007) A gene from the cellulose synthase-like C family encodes a beta-1,4 glucan synthase. Proc Natl Acad Sci U S A **104**: 8550–8555

Cosgrove DJ (2005) Growth of the plant cell wall. Nat Rev Mol Cell Biol **6**: 850–61

Dagel DJ, Liu YS, Zhong L, Luo Y, Himmel ME, Xu Q, Zeng Y, Ding SY, Smith S (2011) In situ imaging of single carbohydrate-binding modules on cellulose microfibrils. J Phys Chem B **115**: 635–641

Dea ICM, Morris ER, Rees DA, Welsh EJ, Barnes H a., Price J (1977) Associations of like and unlike polysaccharides: Mechanism and specificity in galactomannans, interacting bacterial polysaccharides, and related systems. Carbohydr Res **57**: 249–272

Dean G, Cao Y, Xiang D, Provart NJ, Ramsay L, Ahad A, White R, Selvaraj G, Datla R, Haughn G (2011) Analysis of gene expression patterns during seed coat development in Arabidopsis. Mol Plant **4**: 1074–91

Dean GH, Zheng H, Tewari J, Huang J, Young DS, Hwang YT, Western TL, Carpita NC, McCann MC, Mansfield SD, et al (2007) The Arabidopsis MUM2 gene encodes a beta-galactosidase required for the production of seed coat mucilage with correct hydration properties. Plant Cell **19**: 4007–4021

Dhugga KS, Barreiro R, Whitten B, Stecca K, Hazebroek J, Randhawa GS, Dolan M, Kinney AJ, Tomes D, Nichols S, et al (2004) Guar seed beta-mannan synthase is a member of the cellulose synthase super gene family. Science **303**: 363–366

Dunkley TPJ, Hester S, Shadforth IP, Runions J, Weimar T, Hanton SL, Griffin JL, Bessant C, Brandizzi F, Hawes C, et al (2006) Mapping the Arabidopsis organelle proteome. Proc Natl Acad Sci U S A **103**: 6518–6523

Dunkley TPJ, Watson R, Griffin JL, Dupree P, Lilley KS (2004) Localization of organelle proteins by isotope tagging (LOPIT). Mol Cell Proteomics **3**: 1128–1134

Earley KW, Haag JR, Pontes O, Opper K, Juehne T, Song K, Pikaard CS (2006) Gateway-compatible vectors for plant functional genomics and proteomics. Plant J **45**: 616–629

Eda S, Akiyama Y, Katō K, Ishizu A, Nakano J (1985) A galactoglucomannan from cell walls of suspension-cultured tobacco (Nicotiana tabacum) cells. Carbohydr Res **137**: 173–181

Edwards M, Scott C, Gidley MJ, Reid JS (1992) Control of mannose/galactose ratio during galactomannan formation in developing legume seeds. Planta **187**: 67–74

Edwards ME, Dickson CA, Chengappa S, Sidebottom C, Gidley MJ, Reid JSG (1999) Molecular characterisation of a membrane-bound galactosyltransferase of plant cell wall matrix polysaccharide biosynthesis. Plant J **19**: 691–7

Eronen P, Österberg M, Heikkinen S, Tenkanen M, Laine J (2011) Interactions of structurally different hemicelluloses with nanofibrillar cellulose. Carbohydr Polym **86**: 1281–1290

Faik A, Price NJ, Raikhel N V, Keegstra K (2002) An Arabidopsis gene encoding an alpha-xylosyltransferase involved in xyloglucan biosynthesis. Proc Natl Acad Sci U S A **99**: 7797–802

Foster CE, Martin TM, Pauly M (2010) Comprehensive compositional analysis of plant cell walls (Lignocellulosic biomass) part I: lignin. J Vis Exp **37**: e1745

Fraga D, Meulia T, Fenster S (2008) Real-Time PCR. Curr. Protoc. Essent. Lab. Tech. pp 1–33

Geldner N, Dénervaud-Tendon V, Hyman DL, Mayer U, Stierhof Y-D, Chory J (2009) Rapid, combinatorial analysis of membrane compartments in intact plants with a multicolor marker set. Plant J **59**: 169–78

Gibeaut DM, Carpita NC (1991) Tracing cell wall biogenesis in intact cells and plants : selective turnover and alteration of soluble and cell wall polysaccharides in grasses. Plant Physiol **97**: 551–561

Gille S, Cheng K, Skinner ME, Liepman AH, Wilkerson CG, Pauly M (2011) Deep sequencing of voodoo lily (Amorphophallus konjac): An approach to identify relevant genes involved in the synthesis of the hemicellulose glucomannan. Planta **234**: 515–526

Gille S, Hänsel U, Ziemann M, Pauly M (2009) Identification of plant cell wall mutants by means of a forward chemical genetic approach using hydrolases. Proc Natl Acad Sci U S A **106**: 14699–704

Goubet F, Barton CJ, Mortimer JC, Yu X, Zhang Z, Miles GP, Richens J, Liepman AH, Seffen K, Dupree P (2009) Cell wall glucomannan in Arabidopsis is synthesised by CSLA glycosyltransferases, and influences the progression of embryogenesis. Plant J **60**: 527–38

Griffiths J, Šola K, Kushwaha R, Lam P, Tateno M, Young R, Voiniciuc C, Dean G, Shawn DM, DeBolt S, et al (2015) Unidirectional Movement of Cellulose Synthase Complexes in Arabidopsis Seed Coat Epidermal Cells Deposit Cellulose Involved in Mucilage Extrusion, Adherence, and Ray Formation. Plant Physiol **168**: 502–520

Griffiths JS, Tsai AY-L, Xue H, Voiniciuc C, Sola K, Seifert GJ, Mansfield SD, Haughn GW (2014) SALT-OVERLY SENSITIVE5 Mediates Arabidopsis Seed Coat Mucilage Adherence and Organization through Pectins. Plant Physiol **165**: 991–1004

Gutierrez L, Mauriat M, Guénin S, Pelloux J, Lefebvre JF, Louvet R, Rusterucci C, Moritz T, Guerineau F, Bellini C, et al (2008) The lack of a systematic validation of reference genes: A serious pitfall undervalued in reverse transcription-polymerase chain reaction (RT-PCR) analysis in plants. Plant Biotechnol J **6**: 609–618

Handford MG, Baldwin TC, Goubet F, Prime TA, Miles J, Yu X, Dupree P (2003) Localisation and characterisation of cell wall mannan polysaccharides in Arabidopsis thaliana. Planta **218**: 27–36

Harpaz-Saad S, McFarlane HE, Xu S, Divi UK, Forward B, Western TL, Kieber JJ (2011) Cellulose synthesis via the FEI2 RLK/SOS5 pathway and cellulose synthase 5 is required for the structure of seed coat mucilage in Arabidopsis. Plant J **68**: 941–53

Haughn GW, Western TL (2012) Arabidopsis Seed Coat Mucilage is a Specialized Cell Wall that Can be Used as a Model for Genetic Analysis of Plant Cell Wall Structure and Function. Front Plant Sci **3**: 64

Huang J, DeBowles D, Esfandiari E, Dean G, Carpita NC, Haughn GW (2011) The Arabidopsis transcription factor LUH/MUM1 is required for extrusion of seed coat mucilage. Plant Physiol **156**: 491–502

Keegstra K (2010) Plant cell walls. Plant Physiol **154**: 483–6

Keegstra K, Cavalier D (2010) Glycosyltransferases of the GT34 and GT37 Families. Annu Plant Rev **41**: 235–49

Kong Y, Zhou G, Abdeen A, Schafhauser J, Richardson B, Atmodjo M, Jung J, Wicker L, Mohnen D, Western T, et al (2013) GALACTURONOSYLTRANSFERASE-LIKE5 is involved in the production of Arabidopsis seed coat mucilage. Plant Physiol **163**: 1203–17

Kremers G-J, Goedhart J, van Munster EB, Gadella TWJ (2006) Cyan and yellow super fluorescent proteins with improved brightness, protein folding, and FRET Förster radius. Biochemistry **45**: 6570–80

Lao J, Oikawa A, Bromley JR, McInerney P, Suttangkakul A, Smith-Moritz AM, Plahar H, Chiu TY, González Fernández-Niño SM, Ebert B, et al (2014) The plant glycosyltransferase clone collection for functional genomics. Plant J **79**: 517–529

Liepman AH, Nairn CJ, Willats WGT, Sørensen I, Roberts AW, Keegstra K (2007) Functional genomic analysis supports conservation of function among cellulose synthase-like a gene family members and suggests diverse roles of mannans in plants. Plant Physiol **143**: 1881–93

Liepman AH, Wilkerson CG, Keegstra K (2005) Expression of cellulose synthase-like (Csl) genes in insect cells reveals that CslA family members encode mannan synthases. Proc Natl Acad Sci U S A **102**: 2221–6

Liwanag AJM, Ebert B, Verhertbruggen Y, Rennie EA, Rautengarten C, Oikawa A, Andersen MCF, Clausen MH, Scheller HV, Jennifer A, et al (2012) Pectin biosynthesis:

GALS1 in Arabidopsis thaliana is a β-1,4-galactan β-1,4-galactosyltransferase. Plant Cell **24**: 5024–36

Lombard V, Golaconda Ramulu H, Drula E, Coutinho PM, Henrissat B (2014) The carbohydrate-active enzymes database (CAZy) in 2013. Nucleic Acids Res **42**: 490–495

Macquet A, Ralet M-C, Kronenberger J, Marion-Poll A, North HM (2007) In situ, chemical and macromolecular study of the composition of Arabidopsis thaliana seed coat mucilage. Plant Cell Physiol **48**: 984–99

Manzanares P, De Graaff LH, Visser J (1998) Characterization of galactosidases from Aspergillus niger: Purification of a novel alpha-galactosidase activity. Enzyme Microb Technol **22**: 383–390

Marcus SE, Blake AW, Benians TAS, Lee KJD, Poyser C, Donaldson L, Leroux O, Rogowski A, Petersen HL, Boraston A, et al (2010) Restricted access of proteins to mannan polysaccharides in intact plant cell walls. Plant J **64**: 191–203

Mendu V, Griffiths JS, Persson S, Stork J, Downie B, Voiniciuc C, Haughn GW, DeBolt S (2011) Subfunctionalization of cellulose synthases in seed coat epidermal cells mediates secondary radial wall synthesis and mucilage attachment. Plant Physiol **157**: 441–453

Millane RP, Hendrixson TL (1994) Crystal structures of mannan and glucomannans. Carbohydr Polym **25**: 245–251

Mutwil M, Obro J, Willats WGT, Persson S (2008) GeneCAT--novel webtools that combine BLAST and co-expression analyses. Nucleic Acids Res **36**: W320–6

Nebenführ A, Ritzenthaler C, Robinson DG (2002) Brefeldin A: deciphering an enigmatic inhibitor of secretion. Plant Physiol **130**: 1102–1108

Nikolovski N, Rubtsov D, Segura MP, Miles GP, Stevens TJ, Dunkley TPJ, Munro S, Lilley KS, Dupree P (2012) Putative glycosyltransferases and other plant Golgi apparatus proteins are revealed by LOPIT proteomics. Plant Physiol **160**: 1037–51

Nikolovski N, Shliaha P V, Gatto L, Dupree P, Lilley KS (2014) Label free protein quantification for plant Golgi protein localisation and abundance. Plant Physiol **166**: 1033–43

North HM, Berger A, Saez-Aguayo S, Ralet M-C (2014) Understanding polysaccharide production and properties using seed coat mutants: future perspectives for the exploitation of natural variants. Ann Bot **114**: 1251–63

Obayashi T, Okamura Y, Ito S, Tadaka S, Aoki Y, Shirota M, Kinoshita K (2014) ATTED-II in 2014: Evaluation of gene coexpression in agriculturally important plants. Plant Cell Physiol **55**: 1–7

Pattathil S, Avci U, Baldwin D, Swennes AG, McGill J a, Popper Z, Bootten T, Albert A, Davis RH, Chennareddy C, et al (2010) A comprehensive toolkit of plant cell wall glycan-directed monoclonal antibodies. Plant Physiol **153**: 514–25

Pauly M, Gille S, Liu L, Mansoori N, de Souza A, Schultink A, Xiong G (2013) Hemicellulose biosynthesis. Planta **238**: 627–642

Pauly M, Keegstra K (2010) Plant cell wall polymers as precursors for biofuels. Curr Opin Plant Biol **13**: 305–12

Pettolino F a, Walsh C, Fincher GB, Bacic A (2012) Determining the polysaccharide composition of plant cell walls. Nat Protoc **7**: 1590–607

Pfaffl MW (2001) A new mathematical model for relative quantification in real-time RT-PCR. Nucleic Acids Res **29**: e45

Preston RD (1968) Plants without Cellulose. Sci Am **218**: 102–108

Ralet M-C, Tranquet O, Poulain D, Moïse A, Guillon F (2010) Monoclonal antibodies to rhamnogalacturonan I backbone. Planta **231**: 1373–1383

Rautengarten C, Usadel B, Neumetzler L, Hartmann J, Büssis D, Altmann T (2008) A subtilisin-like serine protease essential for mucilage release from Arabidopsis seed coats. Plant J **54**: 466–80

Rennie E a., Hansen SF, Baidoo EEK, Hadi MZ, Keasling JD, Scheller H V. (2012) Three Members of the Arabidopsis Glycosyltransferase Family 8 Are Xylan Glucuronosyltransferases. Plant Physiol **159**: 1408–1417

Rodríguez-Gacio MDC, Iglesias-Fernández R, Carbonero P, Matilla ÁJ (2012) Softening-up mannan-rich cell walls. J Exp Bot **63**: 3975–3988

De Rybel B, van den Berg W, Lokerse A, Liao C-Y, van Mourik H, Möller B, Peris CL, Weijers D (2011) A versatile set of ligation-independent cloning vectors for functional studies in plants. Plant Physiol **156**: 1292–9

Saez-Aguayo S, Ralet M-C, Berger A, Botran L, Ropartz D, Marion-Poll A, North HM (2013) PECTIN METHYLESTERASE INHIBITOR6 promotes Arabidopsis mucilage release by limiting methylesterification of homogalacturonan in seed coat epidermal cells. Plant Cell **25**: 308–23

Scheller HV, Ulvskov P (2010) Hemicelluloses. Annu Rev Plant Biol **61**: 263–289

Schindelin J, Arganda-Carreras I, Frise E, Kaynig V, Longair M, Pietzsch T, Preibisch S, Rueden C, Saalfeld S, Schmid B, et al (2012) Fiji: an open-source platform for biological-image analysis. Nat Methods **9**: 676–682

Schwacke R, Schneider A, van der Graaff E, Fischer K, Catoni E, Desimone M, Frommer WB, Flügge U-I, Kunze R (2003) ARAMEMNON, a novel database for Arabidopsis integral membrane proteins. Plant Physiol **131**: 16–26

Shapiro SS, Wilk MB (1965) An Analysis of Variance Test for Normality (Complete Samples). Biometrika **52**: 591–611

Sims IM, Craik DJ, Bacic A (1997) Structural characterisation of galactoglucomannan secreted by suspension-cultured cells of Nicotiana plumbaginifolia. Carbohydr Res **303**: 79–92

Srivastava M, Kapoor VP (2005) Seed galactomannans: An overview. Chem Biodivers **2**: 295–317

Sullivan S, Ralet M-C, Berger A, Diatloff E, Bischoff V, Gonneau M, Marion-Poll A, North HM (2011) CESA5 is required for the synthesis of cellulose with a role in structuring the adherent mucilage of Arabidopsis seeds. Plant Physiol **156**: 1725–39

Suzuki S, Li L, Sun Y-H, Chiang VL (2006) The cellulose synthase gene superfamily and biochemical functions of xylem-specific cellulose synthase-like genes in Populus trichocarpa. Plant Physiol **142**: 1233–1245

Teh O-K, Moore I (2007) An ARF-GEF acting at the Golgi and in selective endocytosis in polarized plant cells. Nature **448**: 493–496

Updegraff DM (1969) Semimicro determination of cellulose in biological materials. Anal Biochem **32**: 420–424

Urbanowicz BR, Peña MJ, Moniz HA, Moremen KW, York WS (2014) Two Arabidopsis proteins synthesize acetylated xylan in vitro. Plant J **80**: 197–206

Vasilevski A, Giorgi FM, Bertinetti L, Usadel B (2012) LASSO modeling of the Arabidopsis thaliana seed/seedling transcriptome: a model case for detection of novel mucilage and pectin metabolism genes. Mol Biosyst **8**: 2566–74

Voiniciuc C, Dean GH, Griffiths JS, Kirchsteiger K, Hwang YT, Gillett A, Dow G, Western TL, Estelle M, Haughn GW (2013) FLYING SAUCER1 is a transmembrane RING E3 ubiquitin ligase that regulates the degree of pectin methylesterification in Arabidopsis seed mucilage. Plant Cell **25**: 944–59

Voiniciuc C, Yang B, Schmidt M, Günl M, Usadel B (2015) Starting to Gel: How Arabidopsis Seed Coat Epidermal Cells Produce Specialized Secondary Cell Walls. Int J Mol Sci **16**: 3452–3473

Vuttipongchaikij S, Brocklehurst D, Steele-King C, Ashford DA, Gomez LD, McQueen-Mason SJ (2012) Arabidopsis GT34 family contains five xyloglucan α-1,6-xylosyltransferases. New Phytol **195**: 585–95

Wang Y, Alonso AP, Wilkerson CG, Keegstra K (2012a) Deep EST profiling of developing fenugreek endosperm to investigate galactomannan biosynthesis and its regulation. Plant Mol Biol **79**: 243–58

Wang Y, Mortimer JC, Davis J, Dupree P, Keegstra K (2012b) Identification of an additional protein involved in mannan biosynthesis. Plant J 105–117

Warde-Farley D, Donaldson SL, Comes O, Zuberi K, Badrawi R, Chao P, Franz M, Grouios C, Kazi F, Lopes CT, et al (2010) The GeneMANIA prediction server: biological network integration for gene prioritization and predicting gene function. Nucleic Acids Res **38**: W214–20

Weigel D, Glazebrook J (2006) In Planta Transformation of Arabidopsis. Cold Spring Harb Protoc **2006**: pdb.prot4668

Willats WGT, McCartney L, Knox JP (2001) In-situ analysis of pectic polysaccharides in seed mucilage and at the root surface of Arabidopsis thaliana. Planta **213**: 37–44

Winter D, Vinegar B, Nahal H, Ammar R, Wilson G V., Provart NJ (2007) An "electronic fluorescent pictograph" Browser for exploring and analyzing large-scale biological data sets. PLoS One **2**: e718

Yin L, Verhertbruggen Y, Oikawa A, Manisseri C, Knierim B, Prak L, Jensen JK, Knox JP, Auer M, Willats WGT, et al (2011) The cooperative activities of CSLD2, CSLD3, and CSLD5 are required for normal Arabidopsis development. Mol Plant **4**: 1024–37

Yu L, Shi D, Li J, Kong Y, Yu Y, Chai G, Hu R, Wang J, Hahn MG, Zhou G (2014) CSLA2, a Glucomannan Synthase, is Involved in Maintaining Adherent Mucilage Structure in Arabidopsis Seed. Plant Physiol **164**: 1842–1856

FIGURE LEGENDS

Figure 1. Analysis of the *MUCI10* Gene and its Paralog, *GT6.*
(A) *MUCI10* is co-expressed with known mucilage genes. Microarray data was visualized with GeneMANIA using all 14 genes as baits (Warde-Farley et al., 2010). (B) *MUCI10* and *GT6* insertions and RT-PCR amplicons (red arrows). Bars = 200 bp. (C) RT-PCR and (D and E) qRT-PCR analyses of gene expression in siliques. Two wild-type (WT) biological replicates were tested at three stages of development (heart, linear cotyledon, mature green), while all mutants were examined at the linear cotyledon stage. (D and E) show *MUCI10* expression (normalized to *UBQ5*), relative to the first WT in each set. KNAT7 is transcription factor predicted to promote hemicellulose biosynthesis in seed mucilage (Voiniciuc et al., 2015). Bars = mean + SD of four (D) or three (E) technical replicates.

Figure 2. *muci10* and *csla2* Have Equally Compact Mucilage But Distinct Chemical Defects. Pectin released from wild-type (WT) and mutant seeds was stained with RR. Bars = 200 µm (A to D; I to L) or 100 µm (E to H; M to P). (Q) Area of RR-stained mucilage capsules. Bars = mean + SD of five biological replicates (>20 seeds each). (R) Relative composition of total mucilage extracts. Bars = mean + SD of five biological replicates. The "a" marks decreases relative to WT, while "b" shows significant changes from WT and *csla2-3* (*t*-test, $P < 0.05$).

Figure 3. Polysaccharide Structure in Wild-Type and *muci10* Total Mucilage Extracts.
(A) Polysaccharide abundance calculated based on the linkage analysis in Table 2. (B) The frequency of Gal and Man linkages is altered in *muci10-1* mucilage. (C) Quantification of non-galactosylated HM, relative to *csla2-3* mucilage, using the LM22 antibody (Marcus et al., 2010). All bars = mean + SD of three biological replicates, except two for wild type (WT) and *muci10-1* in (C). The "a" marks a significant change from WT (*t*-test, $P < 0.05$). (D) Model of GGM in WT mucilage, showing likely roles of CSLA2, a glucomannan synthase, and MUCI10, a putative α-1,6-galactosyltransferase. Mucilage GGM may also contain a rare β-1,2-Gal residue, added by an unknown enzyme.

Figure 4. Immunolabeling of Pectin and Heteromannan in Extruded Mucilage.
INRA-RU1 labeled RG I (A to F), and LM21 labeled HM (G to L). Each panel is an optical section through a whole seed (green = antibody, magenta = seed intrinsic fluorescence). Asterisks indicate columellae. Bars = 200 μm (A to C; G to I); 50 μm (D to F; J to L)

Figure 5. Mutants With GGM Defects Display Reduced S4B Labeling of Cellulose.
Cellulose distribution in wild-type, *csla2-3* and *muci10-2* mucilage extruded from seeds hydrated in water. S4B signal intensity was visualized with the Thal look-up table in Fiji (A to F), or as magenta (G to I). Bars = 200 μm (A to C); 50 μm (D to F)

Figure 6. Impaired GGM Structure Alters Cellulose and β-Glycans Distribution in Mucilage.
Mucilage was immunolabeled with CBM3a (yellow), which has high affinity for crystalline cellulose. β-glycans were then stained with calcofluor (magenta). Bars = 100 μm.

Figure 7. *MUCI10* Partly Controls Crystalline Cellulose Levels and Mucilage Adherence.
(A to H) Birefringence (arrows) of crystalline cellulose in mucilage. Bars = 0.5 mm (A to F), or 0.2 mm (G and H). (I) Seed crystalline cellulose quantified with the Updegraff assay. (J) The percent of each mucilage sugar that is non-adherent. Bars = mean + SD of three biological replicates (I and J). Letters mark changes from the wild type (*t*-test, $P < 0.05$).

Figure 8. β-Glc, α-Gal and β-Man Linkages Are Required for Seed Mucilage Attachment.
RR staining of pectin after endo-1,4-β-D-glucanase (β-Glc), α-galactosidase (α-Gal) and/or endo-1,4 β-mannanase (β-Man) digestions (50 min, 40°C, pH 4.5). The panels on the right show that *35S:MUCI10-sYFP* (line #1) rescues the sensitivity of *muci10-1* to β-Glc digestion. Only disks remain around seeds after α-Gal and β-Man double digestion (M to O). Bars = 1 mm.

Figure 9. α-Gal and β-Man Linkages Primarily Maintain the Adherence of Pectin, not Cellulose.
After digestion of α-Gal and β-Man linkages in mucilage, pectin was stained with RR (see Figure 8), and cellulose was counter-stained with S4B. Asterisks show that S4B cannot penetrate RR-stained adherent mucilage, and only stained cellulosic rays when pectin was detached. Disks visible with light (arrowheads) were labeled by S4B (arrows). Bars = 100 μm.

Figure 10. *MUCI10* Controls Mucilage Density Independently of Calcium Cross-Links.
(A to F) FITC-Dextran 70 kDa molecules (yellow) were excluded from thin rays (arrowheads), or wide mucilage columns (arrows), but fully penetrated *cesa5-1* mucilage (F). (G to L) The *muci10-1* seeds released more compact mucilage than wild-type when imbibed in water, $CaCl_2$ or EDTA for 60 min, before rinsing with water and staining with RR. Bars = 100 μm.

Figure 11. MUCI10-sYFP Punctae Are Sensitive to BFA and Co-Localize with ST-RFP.

Fluorescent proteins stably expressed in Arabidopsis leaf (A, B; G to I) or hypocotyl (C to F) epidermal cells. Panels show one (A, B; G to I) or three optical slices (C to F; Z-project, max intensity method), and intrinsic chloroplast fluorescence (blue). Wave22Y and ST-RFP are Golgi markers. Arrows show punctae, and arrowheads mark large Brefeldin A (BFA) compartments. Bars = 20 µm (A and B), 50 µm (C to F), or 10 µm (G to I).

Figure 12. MUCI10 Enables Galactosylation of Glucomannan Synthesized by CSLA2.
(A) YFP-tagged MUCI10 at least partially rescued GGM synthesis in four independent *muci10-1* T_1 lines. Only MUCI10 line #1 had Gal content (A), RR staining and mucilage area similar to WT (B to J). In (B to J), colours denote plants homozygous for *muci10-1* (purple) and/or *csla2-3* (green) mutations. Error bars = SD of three biological or technical (only for #1, #2, and *muci10 csla2*) replicates. The "a" marks changes from WT (*t*-test, $P < 0.05$). Scale bars = 100 µm.

Supplemental Figure S1. *MUCI10* and *GT6* Seed Coat eFP Expression Profiles.
(A) *MUCI10* expression during seed development using the eFP Browser and ATH1 microarray data (Winter et al., 2007; Belmonte et al., 2013). *GT6* lacks an ATH1 probe. (B) and (C) Expression at 3, 7, and 11 days post-anthesis (DPA) in dissected seed coats (Dean et al., 2011). Mucilage is produced in wild-type (WT) at 7 DPA, but not in *ap2*, which fails to develop normal epidermal cells. Red numbers indicate significant fold changes in expression (*t*-test, $P < 0.05$).

Supplemental Figure S2. Overview of Fiji Analysis to Quantify RR-Stained Mucilage.
(A) Raw image of RR-stained seeds. This is a small section of a 10.25 x 7.69 mm view of an entire well of a 24-well plate. Two distinct Colour Thresholding parameters were applied in Fiji to select either Mucilage + Seeds (B), or just Seeds (C). Bars = 500 µm.

Supplemental Figure S3. LM21 Labeling of Heteromannan in Extruded Seed Mucilage.
Single optical sections of whole seeds. Col-0 wild-type (WT) is the reference for all mutants shown. Lm-2, Ri-0 and Lc-0 are three natural accessions. WT lacking the primary antibody is shown as a negative control. The higher magnification panels correspond to the samples directly above. Bars = 200 µm (A to C, G to I, K and L); 50 µm (D to F, J).

Supplemental Figure S4. S4B Labeling of Cellulose Is Reduced in *muci10*, *csla2* and *cesa5*.
Single optical sections coloured with the Thal look-up table in Fiji. Calibration bars indicate fluorescence signal intensity. Scale bars = 50 µm.

Supplemental Figure S5. CBM3a Labeling of *muci10* and *csla2* Single and Double Mutants
Single optical sections of whole seeds. Mucilage was immunolabeled with CBM3a (yellow), which has high affinity for crystalline cellulose. β-glycans were then stained with calcofluor (magenta). Bars = 100 µm.

Supplemental Figure S6. β-Glucanase Digestion of Extruded Seed Mucilage.
Seeds were incubated (90 min, 37°C, pH 4.5) with or without 10 units of β-Glucanase (E-CELTR from Megazyme). After rinsing with water, seeds were stained with RR. Bars = 100 µm.

Supplemental Figure S7. Large FITC-Dextran Molecules Cannot Permeate Mucilage.
FITC-Dextrans (yellow) of increasing molecular size are excluded from wild-type (WT) rays (arrowheads) and *muci10* wide mucilage columns (arrows). Bars = 100 µm.

Supplemental Figure S8. GGM Mutants Have Normal Seed Surface Morphology.

Epidermal cell morphology at the edge (A to D) or in the center of seeds (E to H). Four natural Arabidopsis accessions are shown in (I to P). Bars = 50 µm (A to H; M to P); or 200 µm (I to L).

Supplemental Figure S9. LM21 Immunolabeling of Mature Seed Cryo-Sections.
Optical slices (Z-project, max intensity method) of cryo-sectioned seeds showing LM21 signal (green) and calcofluor or propidium iodide (PI) staining (magenta). Only wild-type and *gt6-1* columellae were labeled with LM21 (arrows). Bars = 100 µm (A to D); 50 µm (E to T).

Supplemental Figure S10. *MUCI10* and *GT6* Do Not Affect Stem AIR Composition.
The relative composition of alcohol-insoluble residue (AIR) was isolated from the bottom 3 cm of four-week old stems. Bars = mean + SD of eight biological replicates.

Supplemental Figure S11. GST-MUCI10 and GST-GT6 Galactosyltransferase Assays.
Proteins purified from E. coli were assayed using UDP-Gal (Promega) as a sugar donor and seven different oligosaccharide acceptor substrates from Megazyme. The amount of UDP released from each reaction was quantified using the UDP-Glo assay (Promega). Bars = mean ± SD of two technical replicates. A “no enzyme” control is shown for each substrate.

Table 1. Monosaccharide Composition of Total Mucilage Extracts.

Relative monosaccharide composition (mol %) and total sugars (µg/mg seed) in mucilage extracted by vigorous mixing in water. Values represent the mean ± SD of five biological replicates per genotype.

	Wild Type			*csla2-3*			*muci10-2*			*muci10-2 gt6-1*			*gt6-1*			*gt6-2*		
Rha	44.12	±	1.56	43.00	±	1.82	43.33	±	1.22	43.49	±	2.24	41.64	±	0.86	43.89	±	1.53
Ara	0.93	±	0.05	1.16	±	0.10	1.11	±	0.13	1.19	±	0.18	0.98	±	0.05	0.98	±	0.02
Gal	1.10	±	0.14	0.65	±	0.08	0.70	±	0.11	0.69	±	0.12	1.08	±	0.08	1.01	±	0.06
Glc	0.76	±	0.13	0.33	±	0.13	0.47	±	0.04	0.52	±	0.08	0.71	±	0.07	0.69	±	0.03
Xyl	3.11	±	0.24	3.22	±	0.10	3.30	±	0.29	3.10	±	0.16	3.15	±	0.07	3.11	±	0.15
Man	0.61	±	0.07	0.13	±	0.01	0.30	±	0.01	0.31	±	0.01	0.59	±	0.05	0.57	±	0.03
GalA	49.21	±	1.38	51.33	±	1.72	50.62	±	0.77	50.51	±	1.70	51.69	±	0.85	49.58	±	1.71
Total	39.86	±	3.24	38.35	±	1.98	38.42	±	3.85	43.51	±	2.11	38.84	±	1.82	39.58	±	1.52

Table 2. Linkage Analysis of Total Mucilage Extracts from Wild-Type and *muci10-1* Seeds.

Total mucilage was extracted by vigorous mixing in water. Values represent the relative composition (%) of each linkage ± SD of three biological replicates. The "[a]" indicates significant differences (*t*-test, $P < 0.05$) from the wild type.

Linkage	Wild Type	*muci10-1*
Rhamnose		
t-Rha	0.49 ± 0.19	0.31 ± 0.19
2-Rha	36.81 ± 0.38	36.69 ± 3.30
2,3-Rha	0.66 ± 0.11	0.86 ± 0.42
2,4-Rha	0.85 ± 0.24	1.31 ± 1.15
Arabinose		
t-Ara	0.07 ± 0.03	0.06 ± 0.01
3-Ara	0.41 ± 0.04	0.74 ± 0.29
5-Ara	0.19 ± 0.04	0.23 ± 0.03
Galactose		
t-Gal	0.71 ± 0.09	0.13 ± 0.05 [a]
2-Gal	0.11 ± 0.01	0.03 ± 0.02 [a]
4-Gal	0.11 ± 0.00	0.11 ± 0.04
6-Gal	0.21 ± 0.11	0.17 ± 0.07
2,4-Gal	0.08 ± 0.01	0.08 ± 0.04
4,6-Gal	0.05 ± 0.03	0.03 ± 0.02
3,6-Gal	0.29 ± 0.05	0.55 ± 0.39
Glucose		
t-Glc	0.01 ± 0.01	0.00 ± 0.00
4-Glc	1.07 ± 0.03	0.73 ± 0.10 [a]
3,4-Glc	0.01 ± 0.01	0.02 ± 0.00
4,6-Glc	0.07 ± 0.01	0.06 ± 0.02
Xylose		
t-Xyl	0.43 ± 0.05	0.42 ± 0.06
4-Xyl	1.61 ± 0.11	1.60 ± 0.04
2,4-Xyl	1.33 ± 0.04	1.45 ± 0.12
Mannose		
4-Man	0.25 ± 0.01	0.34 ± 0.03 [a]
4,6-Man	0.53 ± 0.12	0.14 ± 0.09 [a]
Galacturonic Acid		
t-GalA	0.80 ± 0.33	0.56 ± 0.23
4-GalA	51.39 ± 0.66	50.78 ± 0.57
2,4-GalA	0.56 ± 0.11	0.73 ± 0.36
4,6-GalA	1.24 ± 0.16	1.80 ± 1.21

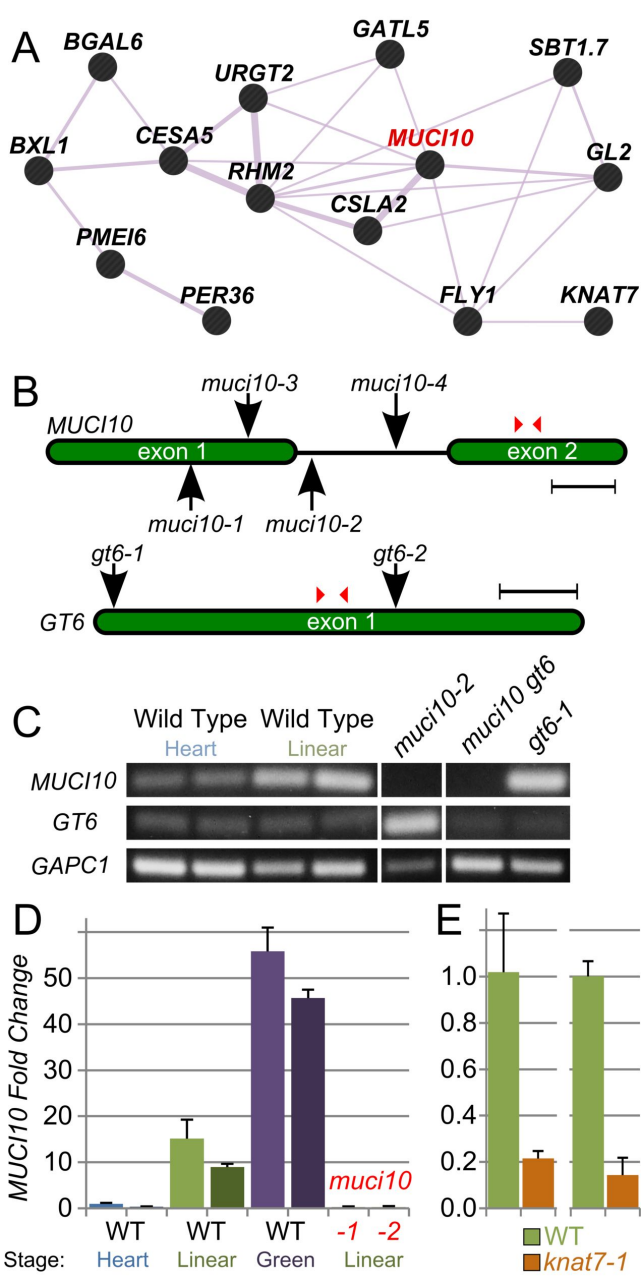
A
BGAL6
GATL5
SBT1.7
URGT2
BXL1
CESA5
MUCI10
GL2
RHM2
CSLA2
PMEI6
PER36
FLY1
KNAT7
B
muci10-3
muci10-4
MUCI10
exon 1
exon 2
muci10-1
muci10-2
gt6-1
gt6-2
GT6
exon 1
C
Wild Type
Heart
Wild Type
Linear
muci10-2
muci10 gt6
gt6-1
MUCI10
GT6
GAPC1
D
MUCI10 Fold Change
0
10
20
30
40
50
muci10
WT
WT
WT
-1
-2
Stage:
Heart
Linear
Green
Linear
E
0.0
0.2
0.4
0.6
0.8
1.0
WT
knat7-1

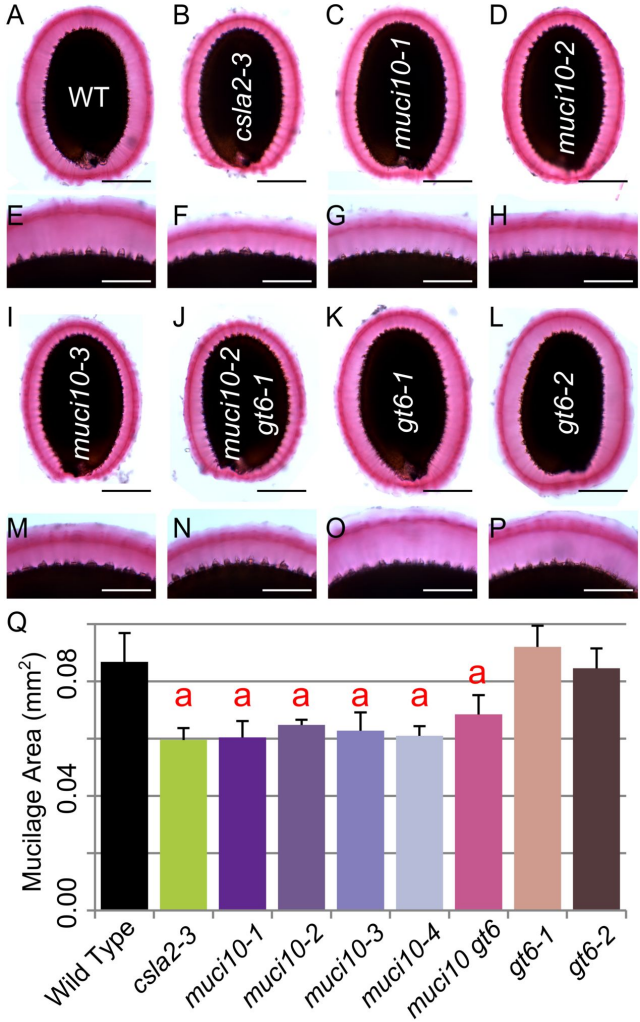
A
WT
B
csla2-3
C
muci10-1
D
muci10-2
E
F
G
H
I
muci10-3
J
muci10-2 gt6-1
K
gt6-1
L
gt6-2
M
N
O
P

Q
Mucilage Area (mm2)
0.00
0.04
0.08
a
a
a
a
a
a
Wild Type
csla2-3
muci10-1
muci10-2
muci10-3
muci10-4
muci10 gt6
gt6-1
gt6-2

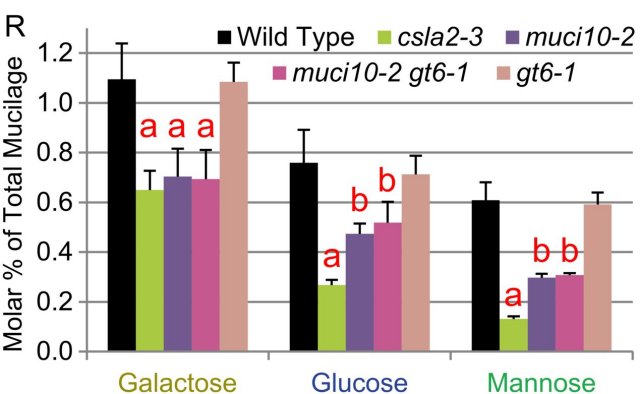
R
Wild Type
csla2-3
muci10-2
muci10-2 gt6-1
gt6-1
Molar % of Total Mucilage
0.0
0.2
0.4
0.6
0.8
1.0
1.2
a a a
a
b
b
a
b b
Galactose
Glucose
Mannose

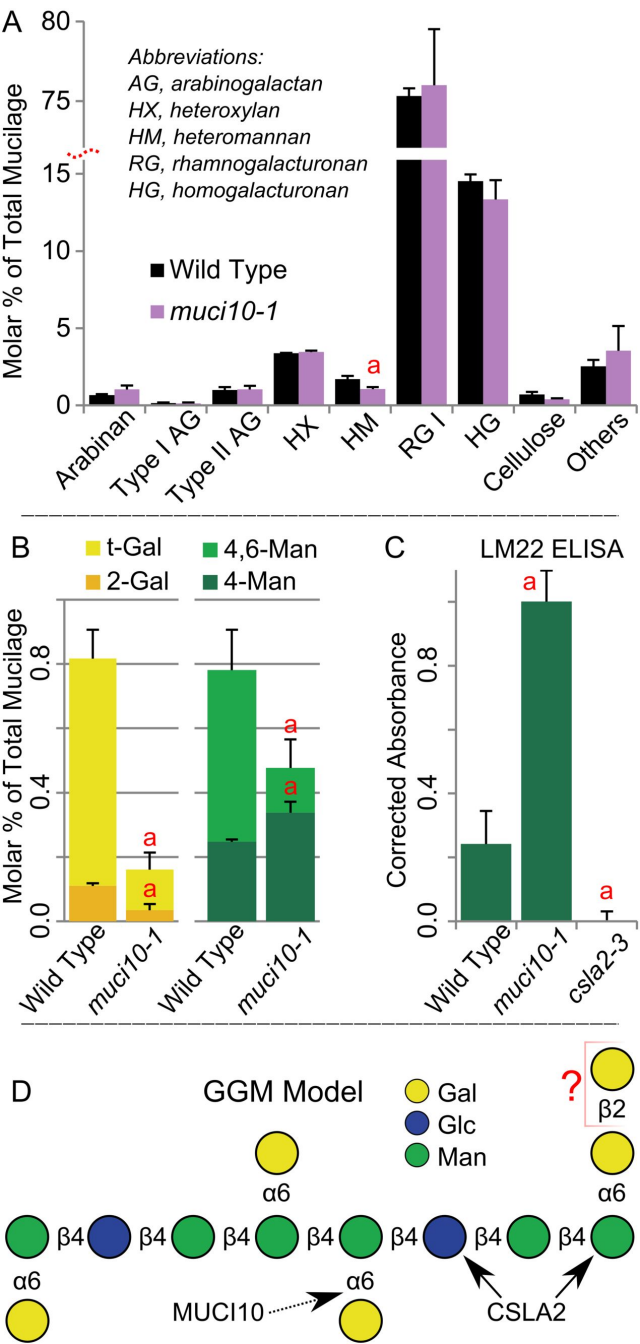
A
Molar % of Total Mucilage
Abbreviations:
AG, arabinogalactan
HX, heteroxylan
HM, heteromannan
RG, rhamnogalacturonan
HG, homogalacturonan
Wild Type
muci10-1
a
Arabinan
Type I AG
Type II AG
HX
HM
RG I
HG
Cellulose
Others
B
t-Gal
2-Gal
4,6-Man
4-Man
Molar % of Total Mucilage
Wild Type
muci10-1
C
LM22 ELISA
Corrected Absorbance
csla2-3
D
GGM Model
Gal
Glc
Man
β2
α6
β4
MUCI10
CSLA2

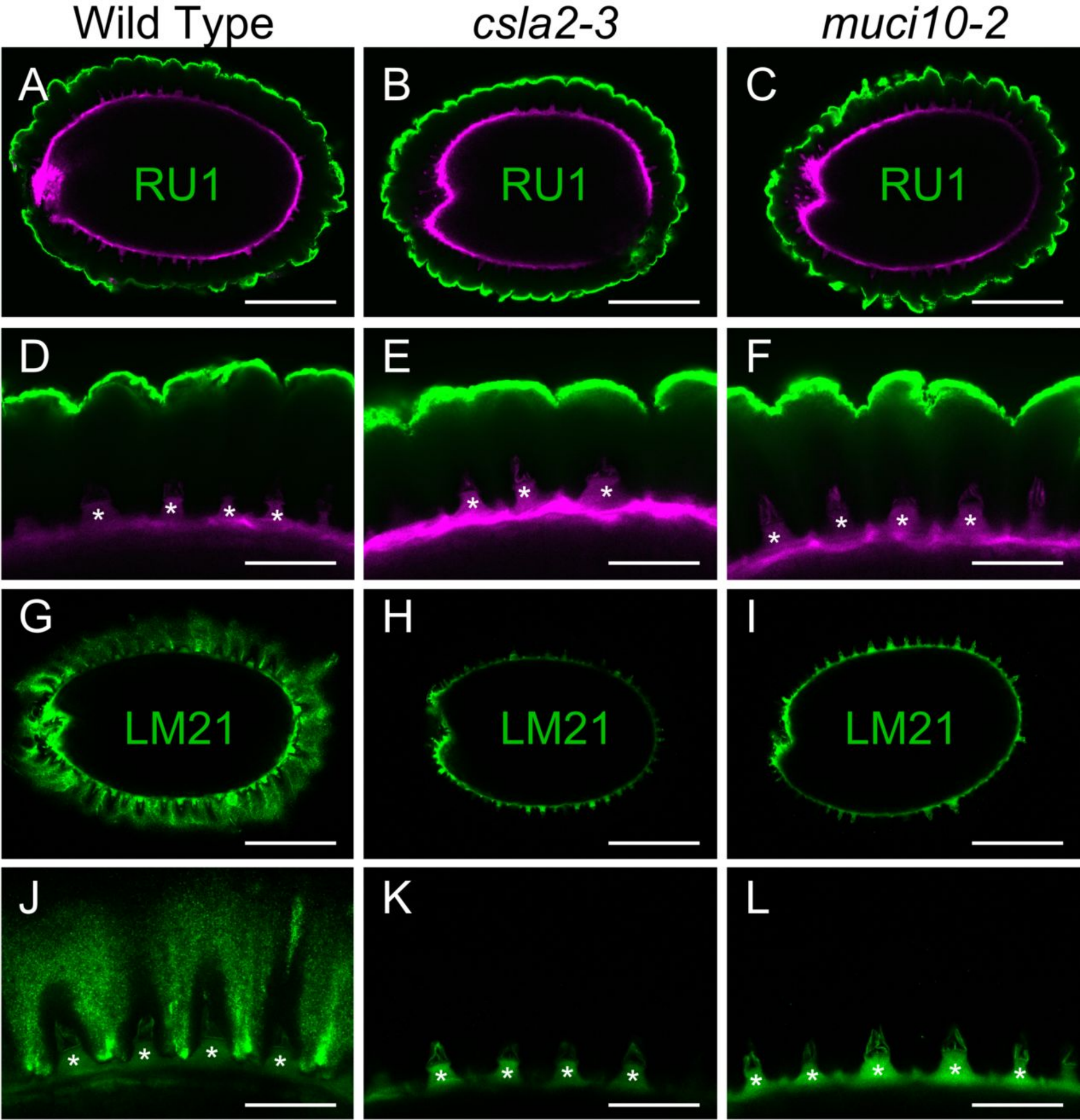
Wild Type
csla2-3
muci10-2
A
RU1
B
RU1
C
RU1
D
E
F
G
LM21
H
LM21
I
LM21
J
K
L

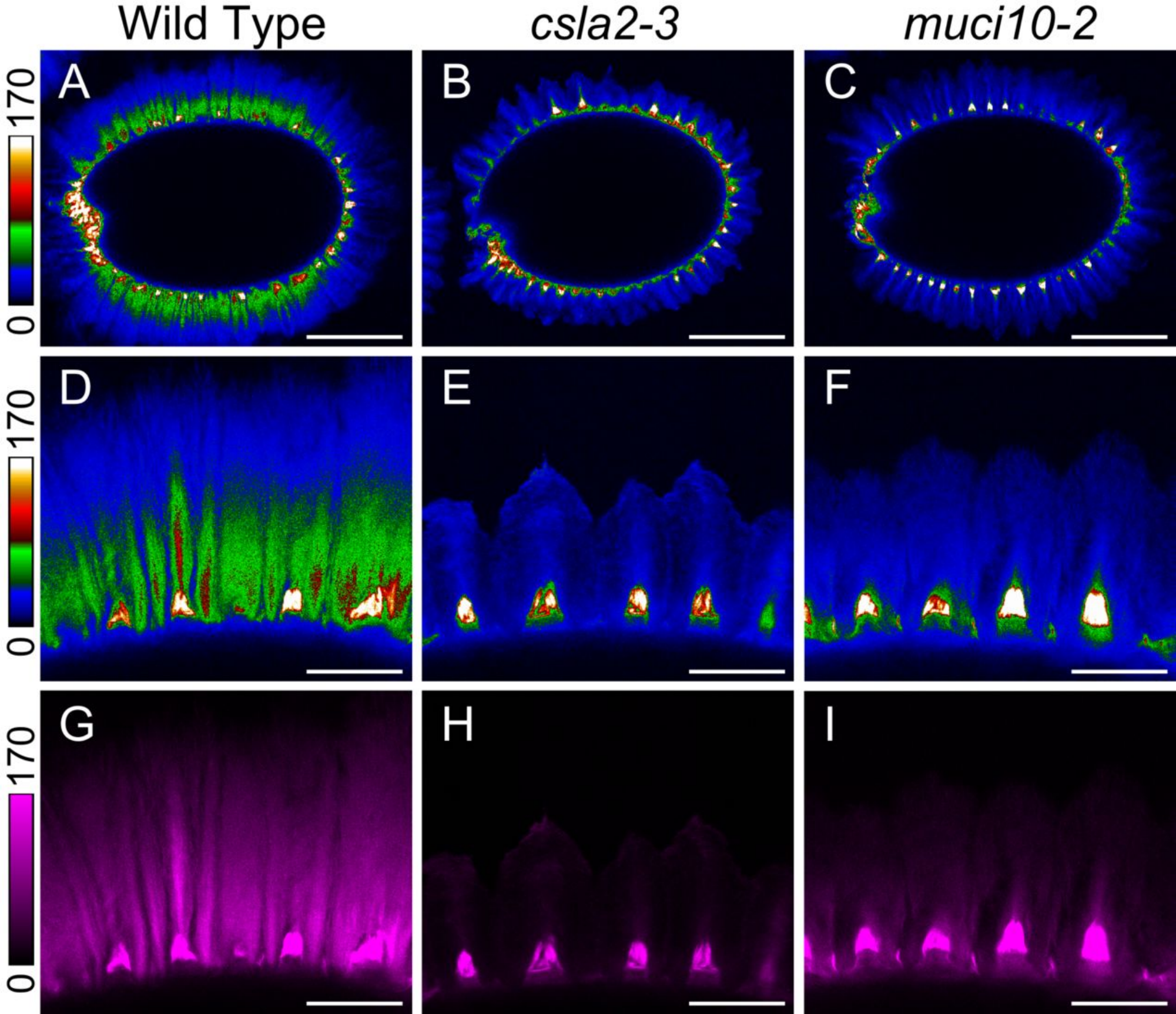
Wild Type
csla2-3
muci10-2
A
B
C
D
E
F
G
H
I
170
0
170
0
170
0

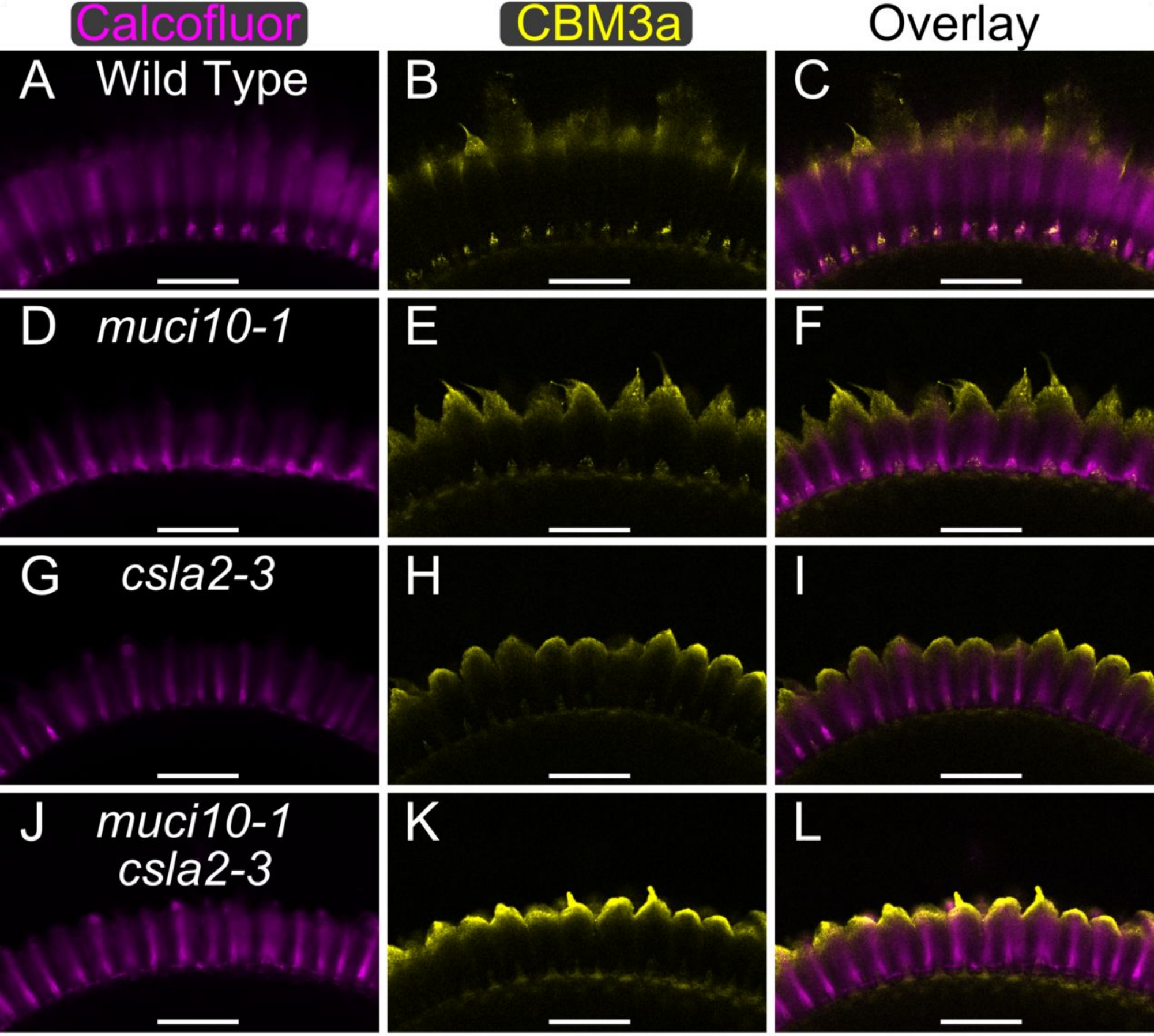
Calcofluor
CBM3a
Overlay
A Wild Type
B
C
D muci10-1
E
F
G csla2-3
H
I
J muci10-1
csla2-3
K
L

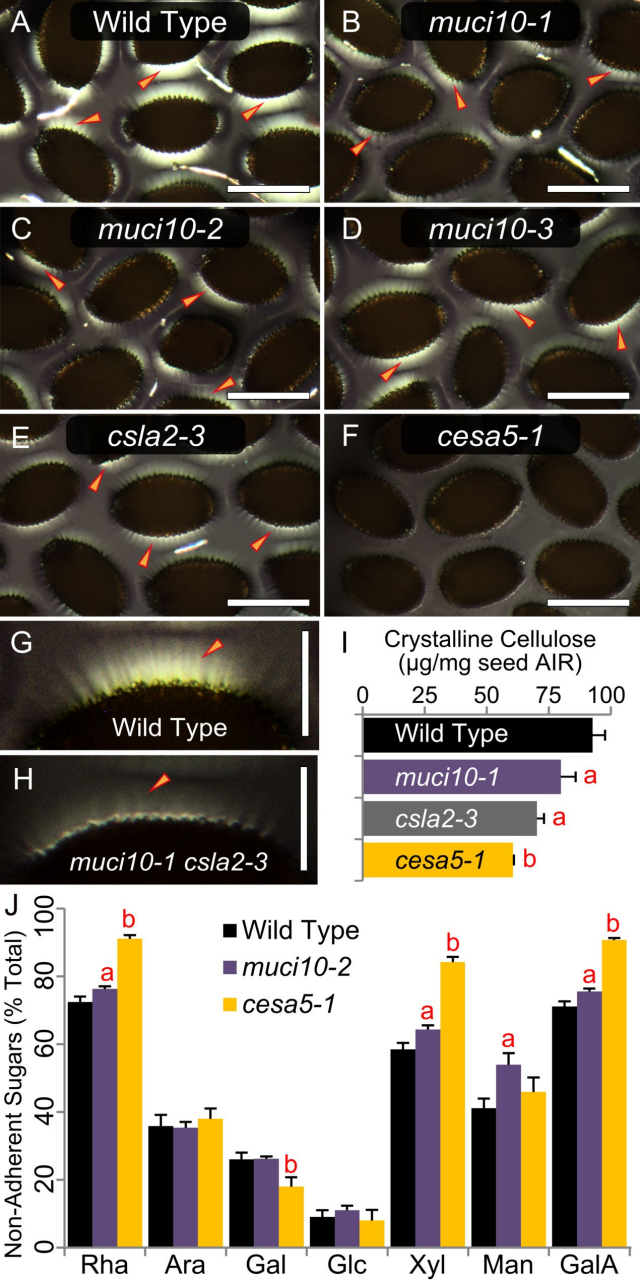
A
Wild Type
B
muci10-1
C
muci10-2
D
muci10-3
E
csla2-3
F
cesa5-1
G
Wild Type
H
muci10-1 csla2-3
I
Crystalline Cellulose
(µg/mg seed AIR)
0
25
50
75
100
Wild Type
muci10-1
a
csla2-3
a
cesa5-1
b
J
Non-Adherent Sugars (% Total)
0
20
40
60
80
100
Wild Type
muci10-2
cesa5-1
Rha
Ara
Gal
Glc
Xyl
Man
GalA

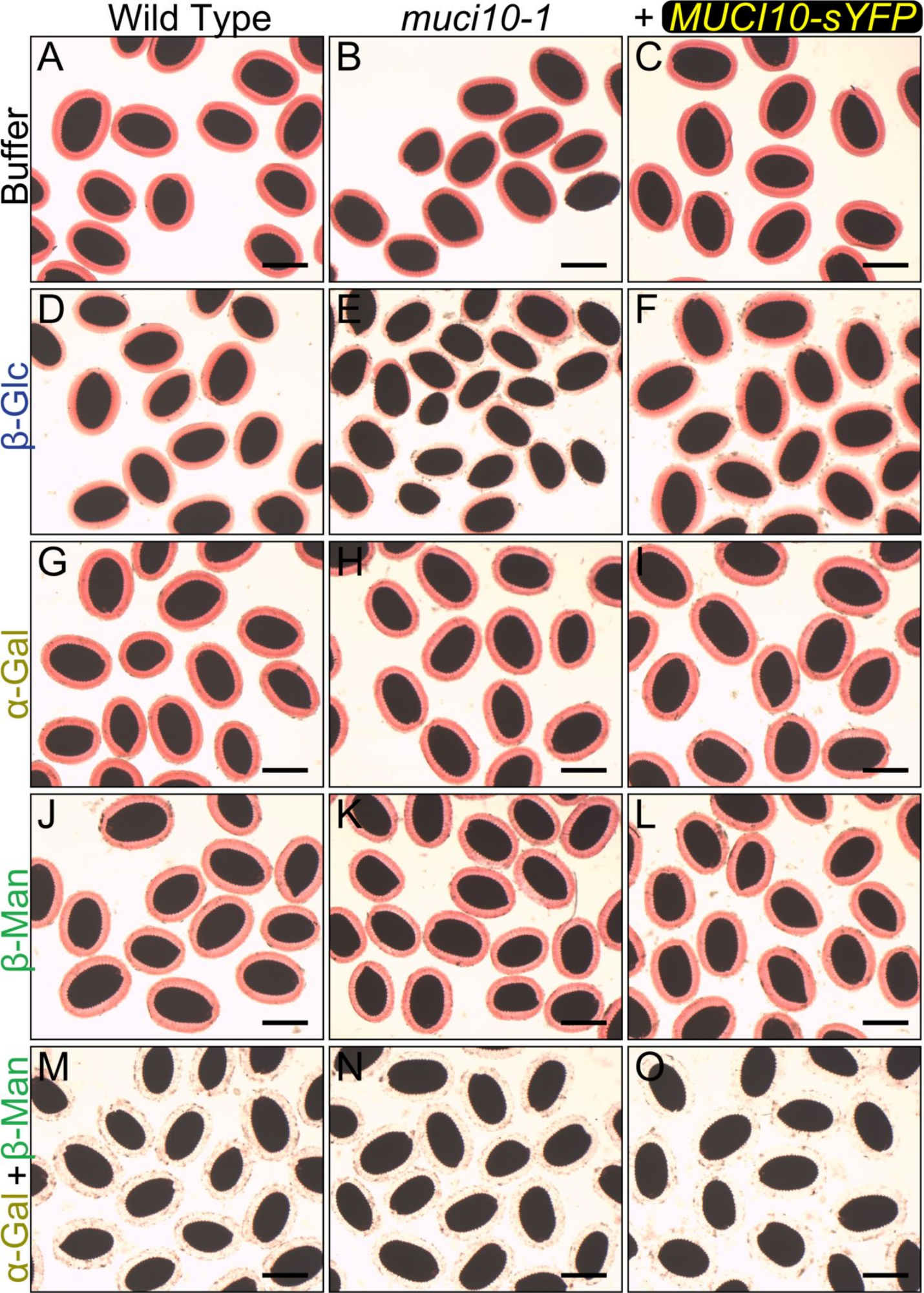
Wild Type
muci10-1
+ MUCI10-sYFP
Buffer
β-Glc
α-Gal
β-Man
α-Gal + β-Man
A
B
C
D
E
F
G
H
I
J
K
L
M
N
O

Transmitted
S4B
Overlay
Wild Type
Buffer Only
A
B
C
Wild Type
α-Gal + β-Man
D
E
F
muci10-1
α-Gal + β-Man
G
H
I
Wild Type
No S4B
J
K
L

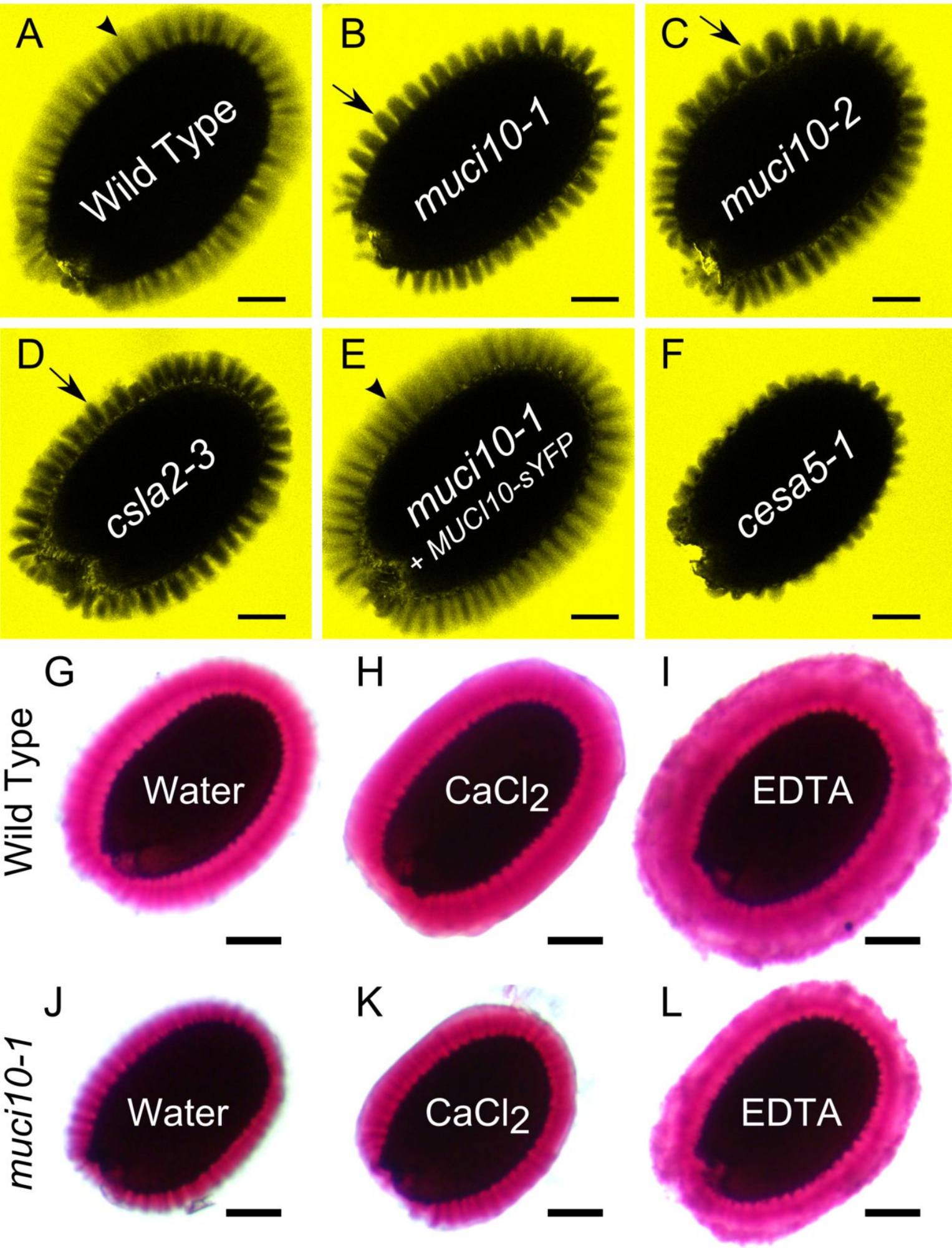
A
Wild Type
B
muci10-1
C
muci10-2
D
csla2-3
E
muci10-1
+ MUCI10-sYFP
F
cesa5-1
G
Water
H
CaCl2
I
EDTA
Wild Type
J
Water
K
CaCl2
L
EDTA
muci10-1

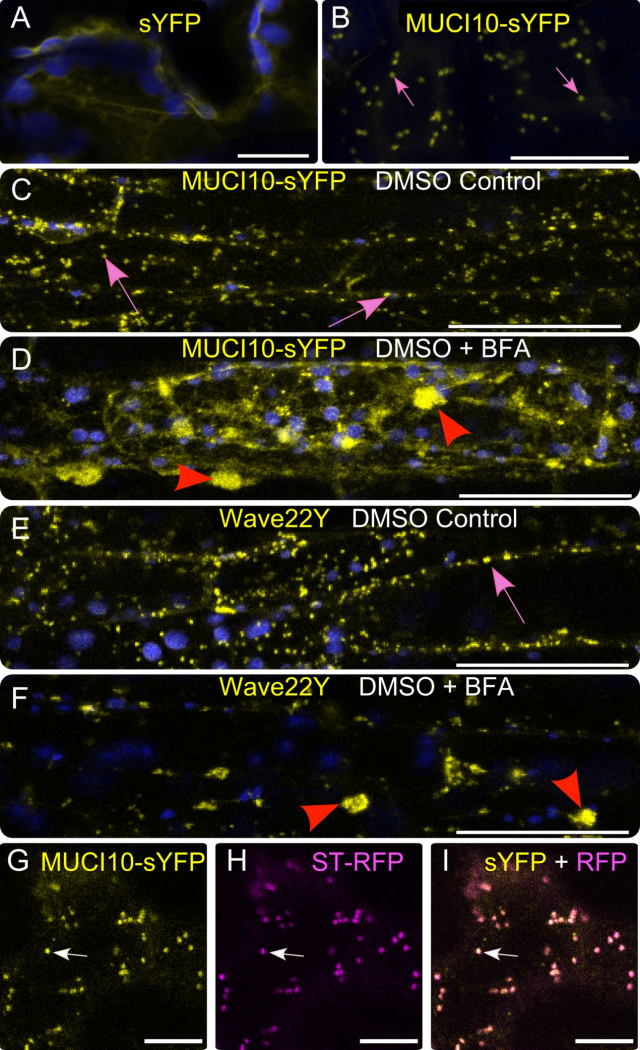
A
sYFP
B
MUCI10-sYFP
C
MUCI10-sYFP DMSO Control
D
MUCI10-sYFP DMSO + BFA
E
Wave22Y DMSO Control
F
Wave22Y DMSO + BFA
G MUCI10-sYFP
H ST-RFP
I sYFP + RFP

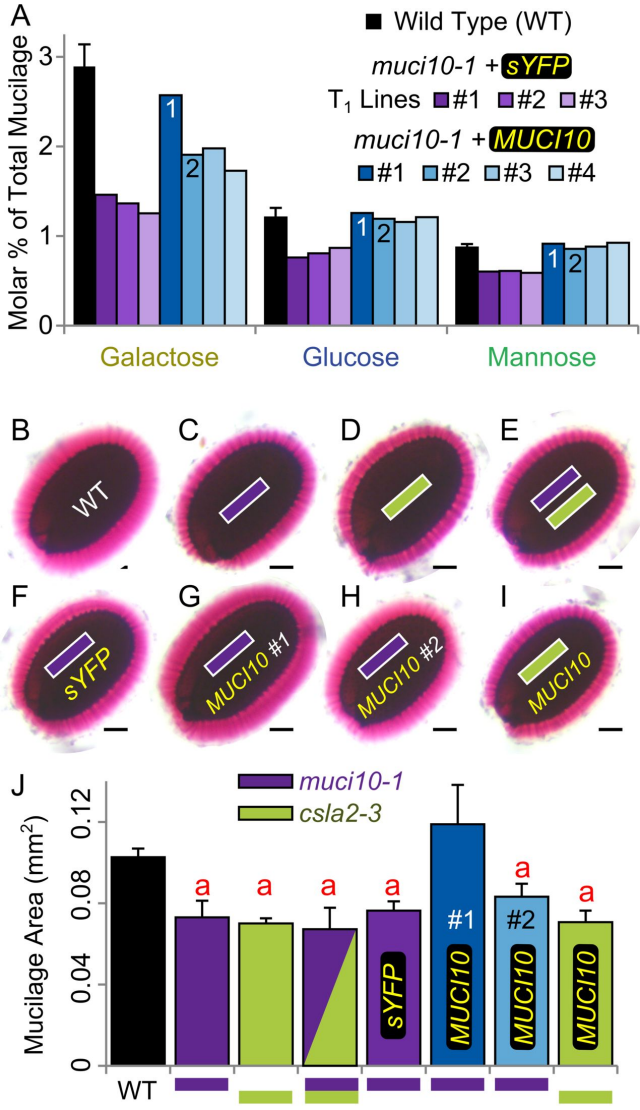
A
Wild Type (WT)
muci10-1 + sYFP
T1 Lines #1 #2 #3
muci10-1 + MUCI10
#1 #2 #3 #4
Molar % of Total Mucilage
0
1
2
3
1
2
1
2
1
2
Galactose
Glucose
Mannose
B
WT
C
D
E
F
sYFP
G
MUCI10 #1
H
MUCI10 #2
I
MUCI10
J
muci10-1
csla2-3
Mucilage Area (mm2)
0
0.04
0.08
0.12
a
a
a
a
a
a
#1
#2
MUCI10
MUCI10
MUCI10
sYFP
WT

Parsed Citations

Alonso JM, Stepanova AN, Leisse TJ, Kim CJ, Chen H, Shinn P, Stevenson DK, Zimmerman J, Barajas P, Cheuk R, et al (2003) Genome-wide insertional mutagenesis of Arabidopsis thaliana. Science 301: 653-657

Pubmed: Author and Title
CrossRef: Author and Title
Google Scholar: Author Only Title Only Author and Title

Anderson CT, Carroll A, Akhmetova L, Somerville C (2010) Real-time imaging of cellulose reorientation during cell wall expansion in Arabidopsis roots. Plant Physiol 152: 787-96

Pubmed: Author and Title
CrossRef: Author and Title
Google Scholar: Author Only Title Only Author and Title

Arvidsson S, Kwasniewski M, Riaño-Pachón DM, Mueller-Roeber B (2008) QuantPrime--a flexible tool for reliable high-throughput primer design for quantitative PCR. BMC Bioinformatics 9: 465

Pubmed: Author and Title
CrossRef: Author and Title
Google Scholar: Author Only Title Only Author and Title

Belmonte MF, Kirkbride RC, Stone SL, Pelletier JM, Bui AQ, Yeung EC, Hashimoto M, Fei J, Harada CM, Munoz MD, et al (2013) Comprehensive developmental profiles of gene activity in regions and subregions of the Arabidopsis seed. Proc Natl Acad Sci U S A 110: E435-44

Pubmed: Author and Title
CrossRef: Author and Title
Google Scholar: Author Only Title Only Author and Title

Benová-Kákosová A, Digonnet C, Goubet F, Ranocha P, Jauneau A, Pesquet E, Barbier O, Zhang Z, Capek P, Dupree P, et al (2006) Galactoglucomannans increase cell population density and alter the protoxylem/metaxylem tracheary element ratio in xylogenic cultures of Zinnia. Plant Physiol 142: 696-709

Pubmed: Author and Title
CrossRef: Author and Title
Google Scholar: Author Only Title Only Author and Title

Ben-Tov D, Abraham Y, Stav S, Thompson K, Loraine A, Elbaum R, De Souza A, Pauly M, Kieber JJ, Harpaz-Saad S (2015) COBRA-LIKE 2, a member of the GPI-anchored COBRA-LIKE family, plays a role in cellulose deposition in Arabidopsis seed coat mucilage secretory cells. Plant Physiol 167: 711-24

Pubmed: Author and Title
CrossRef: Author and Title
Google Scholar: Author Only Title Only Author and Title

Berendzen K, Searle I, Ravenscroft D, Koncz C, Batschauer A, Coupland G, Somssich IE, Ulker B (2005) A rapid and versatile combined DNA/RNA extraction protocol and its application to the analysis of a novel DNA marker set polymorphic between Arabidopsis thaliana ecotypes Col-0 and Landsberg erecta. Plant Methods 1: 4

Pubmed: Author and Title
CrossRef: Author and Title
Google Scholar: Author Only Title Only Author and Title

Bernal AAJ, Yoo CC-M, Mutwil M, Jensen JKJ, Hou G, Blaukopf C, Sørensen I, Blancaflor EB, Scheller HV, Willats WGT (2008) Functional analysis of the cellulose synthase-like genes CSLD1, CSLD2, and CSLD4 in tip-growing Arabidopsis cells. Plant Physiol 148: 1238-53

Pubmed: Author and Title
CrossRef: Author and Title
Google Scholar: Author Only Title Only Author and Title

Blake AW, McCartney L, Flint JE, Bolam DN, Boraston AB, Gilbert HJ, Knox JP (2006) Understanding the biological rationale for the diversity of cellulose-directed carbohydrate-binding modules in prokaryotic enzymes. J Biol Chem 281: 29321-9

Pubmed: Author and Title
CrossRef: Author and Title
Google Scholar: Author Only Title Only Author and Title

Brown C, Leijon F, Bulone V (2012) Radiometric and spectrophotometric in vitro assays of glycosyltransferases involved in plant cell wall carbohydrate biosynthesis. Nat Protoc 7: 1634-50

Pubmed: Author and Title
CrossRef: Author and Title
Google Scholar: Author Only Title Only Author and Title

Burton RA, Fincher GB (2012) Current challenges in cell wall biology in the cereals and grasses. Front Plant Sci 3: 130

Pubmed: Author and Title
CrossRef: Author and Title
Google Scholar: Author Only Title Only Author and Title

Burton RA, Gidley MJ, Fincher GB (2010) Heterogeneity in the chemistry, structure and function of plant cell walls. Nat Chem Biol 6: 724-32

Pubmed: Author and Title
CrossRef: Author and Title
Google Scholar: Author Only Title Only Author and Title

Caffall KH, Pattathil S, Phillips SE, Hahn MG, Mohnen D (2009) Arabidopsis thaliana T-DNA mutants implicate GAUT genes in the

biosynthesis of pectin and xylan in cell walls and seed testa. Mol Plant 2: 1000-14
Pubmed: Author and Title
CrossRef: Author and Title
Google Scholar: Author Only Title Only Author and Title

Cao J, Schneeberger K, Ossowski S, Günther T, Bender S, Fitz J, Koenig D, Lanz C, Stegle O, Lippert C, et al (2011) Whole-genome sequencing of multiple Arabidopsis thaliana populations. Nat Genet 43: 956-63
Pubmed: Author and Title
CrossRef: Author and Title
Google Scholar: Author Only Title Only Author and Title

Carpita N, Tierney M, Campbell M (2001) Molecular biology of the plant cell wall: Searching for the genes that define structure, architecture and dynamics. Plant Mol Biol 47: 1-5
Pubmed: Author and Title
CrossRef: Author and Title
Google Scholar: Author Only Title Only Author and Title

Cavalier DM, Lerouxel O, Neumetzler L, Yamauchi K, Reinecke A, Freshour G, Zabotina OA, Hahn MG, Burgert I, Pauly M, et al (2008) Disrupting two Arabidopsis thaliana xylosyltransferase genes results in plants deficient in xyloglucan, a major primary cell wall component. Plant Cell 20: 1519-37
Pubmed: Author and Title
CrossRef: Author and Title
Google Scholar: Author Only Title Only Author and Title

Chou Y-H, Pogorelko G, Young ZT, Zabotina OA (2014) Protein-Protein Interactions Among Xyloglucan-Synthesizing Enzymes and Formation of Golgi-Localized Multiprotein Complexes. Plant Cell Physiol 56: 255-267
Pubmed: Author and Title
CrossRef: Author and Title
Google Scholar: Author Only Title Only Author and Title

Chou Y-H, Pogorelko G, Zabotina OA (2012) Xyloglucan Xylosyltransferases XXT1, XXT2, and XXT5 and the Glucan Synthase CSLC4 Form Golgi-Localized Multiprotein Complexes. PLANT Physiol 159: 1355-1366
Pubmed: Author and Title
CrossRef: Author and Title
Google Scholar: Author Only Title Only Author and Title

Cocuron J-C, Lerouxel O, Drakakaki G, Alonso AP, Liepman AH, Keegstra K, Raikhel N, Wilkerson CG (2007) A gene from the cellulose synthase-like C family encodes a beta-1,4 glucan synthase. Proc Natl Acad Sci U S A 104: 8550-8555
Pubmed: Author and Title
CrossRef: Author and Title
Google Scholar: Author Only Title Only Author and Title

Cosgrove DJ (2005) Growth of the plant cell wall. Nat Rev Mol Cell Biol 6: 850-61
Pubmed: Author and Title
CrossRef: Author and Title
Google Scholar: Author Only Title Only Author and Title

Dagel DJ, Liu YS, Zhong L, Luo Y, Himmel ME, Xu Q, Zeng Y, Ding SY, Smith S (2011) In situ imaging of single carbohydrate-binding modules on cellulose microfibrils. J Phys Chem B 115: 635-641
Pubmed: Author and Title
CrossRef: Author and Title
Google Scholar: Author Only Title Only Author and Title

Dea ICM, Morris ER, Rees DA, Welsh EJ, Barnes H a., Price J (1977) Associations of like and unlike polysaccharides: Mechanism and specificity in galactomannans, interacting bacterial polysaccharides, and related systems. Carbohydr Res 57: 249-272
Pubmed: Author and Title
CrossRef: Author and Title
Google Scholar: Author Only Title Only Author and Title

Dean G, Cao Y, Xiang D, Provart NJ, Ramsay L, Ahad A, White R, Selvaraj G, Datla R, Haughn G (2011) Analysis of gene expression patterns during seed coat development in Arabidopsis. Mol Plant 4: 1074-91
Pubmed: Author and Title
CrossRef: Author and Title
Google Scholar: Author Only Title Only Author and Title

Dean GH, Zheng H, Tewari J, Huang J, Young DS, Hwang YT, Western TL, Carpita NC, McCann MC, Mansfield SD, et al (2007) The Arabidopsis MUM2 gene encodes a beta-galactosidase required for the production of seed coat mucilage with correct hydration properties. Plant Cell 19: 4007-4021
Pubmed: Author and Title
CrossRef: Author and Title
Google Scholar: Author Only Title Only Author and Title

Dhugga KS, Barreiro R, Whitten B, Stecca K, Hazebroek J, Randhawa GS, Dolan M, Kinney AJ, Tomes D, Nichols S, et al (2004) Guar seed beta-mannan synthase is a member of the cellulose synthase super gene family. Science 303: 363-366
Pubmed: Author and Title
CrossRef: Author and Title
Google Scholar: Author Only Title Only Author and Title

Dunkley TPJ, Hester S, Shadforth IP, Runions J, Weimar T, Hanton SL, Griffin JL, Bessant C, Brandizzi F, Hawes C, et al (2006) Mapping the Arabidopsis organelle proteome. Proc Natl Acad Sci U S A 103: 6518-6523

Pubmed: Author and Title
CrossRef: Author and Title
Google Scholar: Author Only Title Only Author and Title

Dunkley TPJ, Watson R, Griffin JL, Dupree P, Lilley KS (2004) Localization of organelle proteins by isotope tagging (LOPIT). Mol Cell Proteomics 3: 1128-1134
Pubmed: Author and Title
CrossRef: Author and Title
Google Scholar: Author Only Title Only Author and Title

Earley KW, Haag JR, Pontes O, Opper K, Juehne T, Song K, Pikaard CS (2006) Gateway-compatible vectors for plant functional genomics and proteomics. Plant J 45: 616-629
Pubmed: Author and Title
CrossRef: Author and Title
Google Scholar: Author Only Title Only Author and Title

Eda S, Akiyama Y, Kato K, Ishizu A, Nakano J (1985) A galactoglucomannan from cell walls of suspension-cultured tobacco (Nicotiana tabacum) cells. Carbohydr Res 137: 173-181
Pubmed: Author and Title
CrossRef: Author and Title
Google Scholar: Author Only Title Only Author and Title

Edwards M, Scott C, Gidley MJ, Reid JS (1992) Control of mannose/galactose ratio during galactomannan formation in developing legume seeds. Planta 187: 67-74
Pubmed: Author and Title
CrossRef: Author and Title
Google Scholar: Author Only Title Only Author and Title

Edwards ME, Dickson CA, Chengappa S, Sidebottom C, Gidley MJ, Reid JSG (1999) Molecular characterisation of a membrane-bound galactosyltransferase of plant cell wall matrix polysaccharide biosynthesis. Plant J 19: 691-7
Pubmed: Author and Title
CrossRef: Author and Title
Google Scholar: Author Only Title Only Author and Title

Eronen P, Österberg M, Heikkinen S, Tenkanen M, Laine J (2011) Interactions of structurally different hemicelluloses with nanofibrillar cellulose. Carbohydr Polym 86: 1281-1290
Pubmed: Author and Title
CrossRef: Author and Title
Google Scholar: Author Only Title Only Author and Title

Faik A, Price NJ, Raikhel N V, Keegstra K (2002) An Arabidopsis gene encoding an alpha-xylosyltransferase involved in xyloglucan biosynthesis. Proc Natl Acad Sci U S A 99: 7797-802
Pubmed: Author and Title
CrossRef: Author and Title
Google Scholar: Author Only Title Only Author and Title

Foster CE, Martin TM, Pauly M (2010) Comprehensive compositional analysis of plant cell walls (Lignocellulosic biomass) part I: lignin. J Vis Exp 37: e1745
Pubmed: Author and Title
CrossRef: Author and Title
Google Scholar: Author Only Title Only Author and Title

Fraga D, Meulia T, Fenster S (2008) Real-Time PCR. Curr. Protoc. Essent. Lab. Tech. pp 1-33
Pubmed: Author and Title
CrossRef: Author and Title
Google Scholar: Author Only Title Only Author and Title

Geldner N, Dénervaud-Tendon V, Hyman DL, Mayer U, Stierhof Y-D, Chory J (2009) Rapid, combinatorial analysis of membrane compartments in intact plants with a multicolor marker set. Plant J 59: 169-78
Pubmed: Author and Title
CrossRef: Author and Title
Google Scholar: Author Only Title Only Author and Title

Gibeaut DM, Carpita NC (1991) Tracing cell wall biogenesis in intact cells and plants?: selective turnover and alteration of soluble and cell wall polysaccharides in grasses. Plant Physiol 97: 551-561
Pubmed: Author and Title
CrossRef: Author and Title
Google Scholar: Author Only Title Only Author and Title

Gille S, Cheng K, Skinner ME, Liepman AH, Wilkerson CG, Pauly M (2011) Deep sequencing of voodoo lily (Amorphophallus konjac): An approach to identify relevant genes involved in the synthesis of the hemicellulose glucomannan. Planta 234: 515-526
Pubmed: Author and Title
CrossRef: Author and Title
Google Scholar: Author Only Title Only Author and Title

Gille S, Hänsel U, Ziemann M, Pauly M (2009) Identification of plant cell wall mutants by means of a forward chemical genetic approach using hydrolases. Proc Natl Acad Sci U S A 106: 14699-704
Pubmed: Author and Title
CrossRef: Author and Title
Google Scholar: Author Only Title Only Author and Title

Goubet F, Barton CJ, Mortimer JC, Yu X, Zhang Z, Miles GP, Richens J, Liepman AH, Seffen K, Dupree P (2009) Cell wall glucomannan in Arabidopsis is synthesised by CSLA glycosyltransferases, and influences the progression of embryogenesis. Plant J 60: 527-38
Pubmed: Author and Title
CrossRef: Author and Title
Google Scholar: Author Only Title Only Author and Title

Griffiths J, Šola K, Kushwaha R, Lam P, Tateno M, Young R, Voiniciuc C, Dean G, Shawn DM, DeBolt S, et al (2015) Unidirectional Movement of Cellulose Synthase Complexes in Arabidopsis Seed Coat Epidermal Cells Deposit Cellulose Involved in Mucilage Extrusion, Adherence, and Ray Formation. Plant Physiol 168: 502-520
Pubmed: Author and Title
CrossRef: Author and Title
Google Scholar: Author Only Title Only Author and Title

Griffiths JS, Tsai AY-L, Xue H, Voiniciuc C, Sola K, Seifert GJ, Mansfield SD, Haughn GW (2014) SALT-OVERLY SENSITIVE5 Mediates Arabidopsis Seed Coat Mucilage Adherence and Organization through Pectins. Plant Physiol 165: 991-1004
Pubmed: Author and Title
CrossRef: Author and Title
Google Scholar: Author Only Title Only Author and Title

Gutierrez L, Mauriat M, Guénin S, Pelloux J, Lefebvre JF, Louvet R, Rusterucci C, Moritz T, Guerineau F, Bellini C, et al (2008) The lack of a systematic validation of reference genes: A serious pitfall undervalued in reverse transcription-polymerase chain reaction (RT-PCR) analysis in plants. Plant Biotechnol J 6: 609-618
Pubmed: Author and Title
CrossRef: Author and Title
Google Scholar: Author Only Title Only Author and Title

Handford MG, Baldwin TC, Goubet F, Prime TA, Miles J, Yu X, Dupree P (2003) Localisation and characterisation of cell wall mannan polysaccharides in Arabidopsis thaliana. Planta 218: 27-36
Pubmed: Author and Title
CrossRef: Author and Title
Google Scholar: Author Only Title Only Author and Title

Harpaz-Saad S, McFarlane HE, Xu S, Divi UK, Forward B, Western TL, Kieber JJ (2011) Cellulose synthesis via the FEI2 RLK/SOS5 pathway and cellulose synthase 5 is required for the structure of seed coat mucilage in Arabidopsis. Plant J 68: 941-53
Pubmed: Author and Title
CrossRef: Author and Title
Google Scholar: Author Only Title Only Author and Title

Haughn GW, Western TL (2012) Arabidopsis Seed Coat Mucilage is a Specialized Cell Wall that Can be Used as a Model for Genetic Analysis of Plant Cell Wall Structure and Function. Front Plant Sci 3: 64
Pubmed: Author and Title
CrossRef: Author and Title
Google Scholar: Author Only Title Only Author and Title

Huang J, DeBowles D, Esfandiari E, Dean G, Carpita NC, Haughn GW (2011) The Arabidopsis transcription factor LUH/MUM1 is required for extrusion of seed coat mucilage. Plant Physiol 156: 491-502
Pubmed: Author and Title
CrossRef: Author and Title
Google Scholar: Author Only Title Only Author and Title

Keegstra K (2010) Plant cell walls. Plant Physiol 154: 483-6
Pubmed: Author and Title
CrossRef: Author and Title
Google Scholar: Author Only Title Only Author and Title

Keegstra K, Cavalier D (2010) Glycosyltransferases of the GT34 and GT37 Families. Annu Plant Rev 41: 235-49
Pubmed: Author and Title
CrossRef: Author and Title
Google Scholar: Author Only Title Only Author and Title

Kong Y, Zhou G, Abdeen A, Schafhauser J, Richardson B, Atmodjo M, Jung J, Wicker L, Mohnen D, Western T, et al (2013) GALACTURONOSYLTRANSFERASE-LIKE5 is involved in the production of Arabidopsis seed coat mucilage. Plant Physiol 163: 1203-17
Pubmed: Author and Title
CrossRef: Author and Title
Google Scholar: Author Only Title Only Author and Title

Kremers G-J, Goedhart J, van Munster EB, Gadella TWJ (2006) Cyan and yellow super fluorescent proteins with improved brightness, protein folding, and FRET Förster radius. Biochemistry 45: 6570-80
Pubmed: Author and Title
CrossRef: Author and Title
Google Scholar: Author Only Title Only Author and Title

Lao J, Oikawa A, Bromley JR, McInerney P, Suttangkakul A, Smith-Moritz AM, Plahar H, Chiu TY, González Fernández-Niño SM, Ebert B, et al (2014) The plant glycosyltransferase clone collection for functional genomics. Plant J 79: 517-529
Pubmed: Author and Title
CrossRef: Author and Title
Google Scholar: Author Only Title Only Author and Title

Liepman AH, Nairn CJ, Willats WGT, Sørensen I, Roberts AW, Keegstra K (2007) Functional genomic analysis supports conservation of function among cellulose synthase-like a gene family members and suggests diverse roles of mannans in plants. Plant Physiol 143: 1881-93
Pubmed: Author and Title
CrossRef: Author and Title
Google Scholar: Author Only Title Only Author and Title

Liepman AH, Wilkerson CG, Keegstra K (2005) Expression of cellulose synthase-like (Csl) genes in insect cells reveals that CslA family members encode mannan synthases. Proc Natl Acad Sci U S A 102: 2221-6
Pubmed: Author and Title
CrossRef: Author and Title
Google Scholar: Author Only Title Only Author and Title

Liwanag AJM, Ebert B, Verhertbruggen Y, Rennie EA, Rautengarten C, Oikawa A, Andersen MCF, Clausen MH, Scheller HV, Jennifer A, et al (2012) Pectin biosynthesis: GALS1 in Arabidopsis thaliana is a ß-1,4-galactan ß-1,4-galactosyltransferase. Plant Cell 24: 5024-36
Pubmed: Author and Title
CrossRef: Author and Title
Google Scholar: Author Only Title Only Author and Title

Lombard V, Golaconda Ramulu H, Drula E, Coutinho PM, Henrissat B (2014) The carbohydrate-active enzymes database (CAZy) in 2013. Nucleic Acids Res 42: 490-495
Pubmed: Author and Title
CrossRef: Author and Title
Google Scholar: Author Only Title Only Author and Title

Macquet A, Ralet M-C, Kronenberger J, Marion-Poll A, North HM (2007) In situ, chemical and macromolecular study of the composition of Arabidopsis thaliana seed coat mucilage. Plant Cell Physiol 48: 984-99
Pubmed: Author and Title
CrossRef: Author and Title
Google Scholar: Author Only Title Only Author and Title

Manzanares P, De Graaff LH, Visser J (1998) Characterization of galactosidases from Aspergillus niger: Purification of a novel alpha-galactosidase activity. Enzyme Microb Technol 22: 383-390
Pubmed: Author and Title
CrossRef: Author and Title
Google Scholar: Author Only Title Only Author and Title

Marcus SE, Blake AW, Benians TAS, Lee KJD, Poyser C, Donaldson L, Leroux O, Rogowski A, Petersen HL, Boraston A, et al (2010) Restricted access of proteins to mannan polysaccharides in intact plant cell walls. Plant J 64: 191-203
Pubmed: Author and Title
CrossRef: Author and Title
Google Scholar: Author Only Title Only Author and Title

Mendu V, Griffiths JS, Persson S, Stork J, Downie B, Voiniciuc C, Haughn GW, DeBolt S (2011) Subfunctionalization of cellulose synthases in seed coat epidermal cells mediates secondary radial wall synthesis and mucilage attachment. Plant Physiol 157: 441-453
Pubmed: Author and Title
CrossRef: Author and Title
Google Scholar: Author Only Title Only Author and Title

Millane RP, Hendrixson TL (1994) Crystal structures of mannan and glucomannans. Carbohydr Polym 25: 245-251
Pubmed: Author and Title
CrossRef: Author and Title
Google Scholar: Author Only Title Only Author and Title

Mutwil M, Obro J, Willats WGT, Persson S (2008) GeneCAT--novel webtools that combine BLAST and co-expression analyses. Nucleic Acids Res 36: W320-6
Pubmed: Author and Title
CrossRef: Author and Title
Google Scholar: Author Only Title Only Author and Title

Nebenführ A, Ritzenthaler C, Robinson DG (2002) Brefeldin A: deciphering an enigmatic inhibitor of secretion. Plant Physiol 130: 1102-1108
Pubmed: Author and Title
CrossRef: Author and Title
Google Scholar: Author Only Title Only Author and Title

Nikolovski N, Rubtsov D, Segura MP, Miles GP, Stevens TJ, Dunkley TPJ, Munro S, Lilley KS, Dupree P (2012) Putative glycosyltransferases and other plant Golgi apparatus proteins are revealed by LOPIT proteomics. Plant Physiol 160: 1037-51
Pubmed: Author and Title
CrossRef: Author and Title
Google Scholar: Author Only Title Only Author and Title

Nikolovski N, Shliaha P V, Gatto L, Dupree P, Lilley KS (2014) Label free protein quantification for plant Golgi protein localisation and abundance. Plant Physiol 166: 1033-43
Pubmed: Author and Title
CrossRef: Author and Title
Google Scholar: Author Only Title Only Author and Title

North HM, Berger A, Saez-Aguayo S, Ralet M-C (2014) Understanding polysaccharide production and properties using seed coat mutants: future perspectives for the exploitation of natural variants. Ann Bot 114: 1251-63
Pubmed: Author and Title
CrossRef: Author and Title
Google Scholar: Author Only Title Only Author and Title

Obayashi T, Okamura Y, Ito S, Tadaka S, Aoki Y, Shirota M, Kinoshita K (2014) ATTED-II in 2014: Evaluation of gene coexpression in agriculturally important plants. Plant Cell Physiol 55: 1-7
Pubmed: Author and Title
CrossRef: Author and Title
Google Scholar: Author Only Title Only Author and Title

Pattathil S, Avci U, Baldwin D, Swennes AG, McGill J a, Popper Z, Bootten T, Albert A, Davis RH, Chennareddy C, et al (2010) A comprehensive toolkit of plant cell wall glycan-directed monoclonal antibodies. Plant Physiol 153: 514-25
Pubmed: Author and Title
CrossRef: Author and Title
Google Scholar: Author Only Title Only Author and Title

Pauly M, Gille S, Liu L, Mansoori N, de Souza A, Schultink A, Xiong G (2013) Hemicellulose biosynthesis. Planta 238: 627-642
Pubmed: Author and Title
CrossRef: Author and Title
Google Scholar: Author Only Title Only Author and Title

Pauly M, Keegstra K (2010) Plant cell wall polymers as precursors for biofuels. Curr Opin Plant Biol 13: 305-12
Pubmed: Author and Title
CrossRef: Author and Title
Google Scholar: Author Only Title Only Author and Title

Pettolino F a, Walsh C, Fincher GB, Bacic A (2012) Determining the polysaccharide composition of plant cell walls. Nat Protoc 7: 1590-607
Pubmed: Author and Title
CrossRef: Author and Title
Google Scholar: Author Only Title Only Author and Title

Pfaffl MW (2001) A new mathematical model for relative quantification in real-time RT-PCR. Nucleic Acids Res 29: e45
Pubmed: Author and Title
CrossRef: Author and Title
Google Scholar: Author Only Title Only Author and Title

Preston RD (1968) Plants without Cellulose. Sci Am 218: 102-108
Pubmed: Author and Title
CrossRef: Author and Title
Google Scholar: Author Only Title Only Author and Title

Ralet M-C, Tranquet O, Poulain D, Moïse A, Guillon F (2010) Monoclonal antibodies to rhamnogalacturonan I backbone. Planta 231: 1373-1383
Pubmed: Author and Title
CrossRef: Author and Title
Google Scholar: Author Only Title Only Author and Title

Rautengarten C, Usadel B, Neumetzler L, Hartmann J, Büssis D, Altmann T (2008) A subtilisin-like serine protease essential for mucilage release from Arabidopsis seed coats. Plant J 54: 466-80
Pubmed: Author and Title
CrossRef: Author and Title
Google Scholar: Author Only Title Only Author and Title

Rennie E a., Hansen SF, Baidoo EEK, Hadi MZ, Keasling JD, Scheller H V. (2012) Three Members of the Arabidopsis Glycosyltransferase Family 8 Are Xylan Glucuronosyltransferases. Plant Physiol 159: 1408-1417
Pubmed: Author and Title
CrossRef: Author and Title
Google Scholar: Author Only Title Only Author and Title

Rodríguez-Gacio MDC, Iglesias-Fernández R, Carbonero P, Matilla ÁJ (2012) Softening-up mannan-rich cell walls. J Exp Bot 63: 3975-3988
Pubmed: Author and Title
CrossRef: Author and Title
Google Scholar: Author Only Title Only Author and Title

De Rybel B, van den Berg W, Lokerse A, Liao C-Y, van Mourik H, Möller B, Peris CL, Weijers D (2011) A versatile set of ligation-independent cloning vectors for functional studies in plants. Plant Physiol 156: 1292-9
Pubmed: Author and Title
CrossRef: Author and Title
Google Scholar: Author Only Title Only Author and Title

Saez-Aguayo S, Ralet M-C, Berger A, Botran L, Ropartz D, Marion-Poll A, North HM (2013) PECTIN METHYLESTERASE INHIBITOR6 promotes Arabidopsis mucilage release by limiting methylesterification of homogalacturonan in seed coat epidermal cells. Plant Cell 25: 308-23
Pubmed: Author and Title
CrossRef: Author and Title
Google Scholar: Author Only Title Only Author and Title

Scheller HV, Ulvskov P (2010) Hemicelluloses. Annu Rev Plant Biol 61: 263-289
Pubmed: Author and Title
CrossRef: Author and Title
Google Scholar: Author Only Title Only Author and Title

Schindelin J, Arganda-Carreras I, Frise E, Kaynig V, Longair M, Pietzsch T, Preibisch S, Rueden C, Saalfeld S, Schmid B, et al (2012) Fiji: an open-source platform for biological-image analysis. Nat Methods 9: 676-682
Pubmed: Author and Title
CrossRef: Author and Title
Google Scholar: Author Only Title Only Author and Title

Schwacke R, Schneider A, van der Graaff E, Fischer K, Catoni E, Desimone M, Frommer WB, Flügge U-I, Kunze R (2003) ARAMEMNON, a novel database for Arabidopsis integral membrane proteins. Plant Physiol 131: 16-26
Pubmed: Author and Title
CrossRef: Author and Title
Google Scholar: Author Only Title Only Author and Title

Shapiro SS, Wilk MB (1965) An Analysis of Variance Test for Normality (Complete Samples). Biometrika 52: 591-611
Pubmed: Author and Title
CrossRef: Author and Title
Google Scholar: Author Only Title Only Author and Title

Sims IM, Craik DJ, Bacic A (1997) Structural characterisation of galactoglucomannan secreted by suspension-cultured cells of Nicotiana plumbaginifolia. Carbohydr Res 303: 79-92
Pubmed: Author and Title
CrossRef: Author and Title
Google Scholar: Author Only Title Only Author and Title

Srivastava M, Kapoor VP (2005) Seed galactomannans: An overview. Chem Biodivers 2: 295-317
Pubmed: Author and Title
CrossRef: Author and Title
Google Scholar: Author Only Title Only Author and Title

Sullivan S, Ralet M-C, Berger A, Diatloff E, Bischoff V, Gonneau M, Marion-Poll A, North HM (2011) CESA5 is required for the synthesis of cellulose with a role in structuring the adherent mucilage of Arabidopsis seeds. Plant Physiol 156: 1725-39
Pubmed: Author and Title
CrossRef: Author and Title
Google Scholar: Author Only Title Only Author and Title

Suzuki S, Li L, Sun Y-H, Chiang VL (2006) The cellulose synthase gene superfamily and biochemical functions of xylem-specific cellulose synthase-like genes in Populus trichocarpa. Plant Physiol 142: 1233-1245
Pubmed: Author and Title
CrossRef: Author and Title
Google Scholar: Author Only Title Only Author and Title

Teh O-K, Moore I (2007) An ARF-GEF acting at the Golgi and in selective endocytosis in polarized plant cells. Nature 448: 493-496
Pubmed: Author and Title
CrossRef: Author and Title
Google Scholar: Author Only Title Only Author and Title

Updegraff DM (1969) Semimicro determination of cellulose in biological materials. Anal Biochem 32: 420-424
Pubmed: Author and Title
CrossRef: Author and Title
Google Scholar: Author Only Title Only Author and Title

Urbanowicz BR, Peña MJ, Moniz HA, Moremen KW, York WS (2014) Two Arabidopsis proteins synthesize acetylated xylan in vitro. Plant J 80: 197-206
Pubmed: Author and Title
CrossRef: Author and Title
Google Scholar: Author Only Title Only Author and Title

Vasilevski A, Giorgi FM, Bertinetti L, Usadel B (2012) LASSO modeling of the Arabidopsis thaliana seed/seedling transcriptome: a model case for detection of novel mucilage and pectin metabolism genes. Mol Biosyst 8: 2566-74
Pubmed: Author and Title
CrossRef: Author and Title
Google Scholar: Author Only Title Only Author and Title

Voiniciuc C, Dean GH, Griffiths JS, Kirchsteiger K, Hwang YT, Gillett A, Dow G, Western TL, Estelle M, Haughn GW (2013) FLYING SAUCER1 is a transmembrane RING E3 ubiquitin ligase that regulates the degree of pectin methylesterification in Arabidopsis seed mucilage. Plant Cell 25: 944-59
Pubmed: Author and Title
CrossRef: Author and Title
Google Scholar: Author Only Title Only Author and Title

Voiniciuc C, Yang B, Schmidt M, Günl M, Usadel B (2015) Starting to Gel: How Arabidopsis Seed Coat Epidermal Cells Produce Specialized Secondary Cell Walls. Int J Mol Sci 16: 3452-3473
Pubmed: Author and Title
CrossRef: Author and Title
Google Scholar: Author Only Title Only Author and Title

Vuttipongchaikij S, Brocklehurst D, Steele-King C, Ashford DA, Gomez LD, McQueen-Mason SJ (2012) Arabidopsis GT34 family

contains five xyloglucan a-1,6-xylosyltransferases. New Phytol 195: 585-95
Pubmed: Author and Title
CrossRef: Author and Title
Google Scholar: Author Only Title Only Author and Title

Wang Y, Alonso AP, Wilkerson CG, Keegstra K (2012a) Deep EST profiling of developing fenugreek endosperm to investigate galactomannan biosynthesis and its regulation. Plant Mol Biol 79: 243-58
Pubmed: Author and Title
CrossRef: Author and Title
Google Scholar: Author Only Title Only Author and Title

Wang Y, Mortimer JC, Davis J, Dupree P, Keegstra K (2012b) Identification of an additional protein involved in mannan biosynthesis. Plant J 105-117
Pubmed: Author and Title
CrossRef: Author and Title
Google Scholar: Author Only Title Only Author and Title

Warde-Farley D, Donaldson SL, Comes O, Zuberi K, Badrawi R, Chao P, Franz M, Grouios C, Kazi F, Lopes CT, et al (2010) The GeneMANIA prediction server: biological network integration for gene prioritization and predicting gene function. Nucleic Acids Res 38: W214-20
Pubmed: Author and Title
CrossRef: Author and Title
Google Scholar: Author Only Title Only Author and Title

Weigel D, Glazebrook J (2006) In Planta Transformation of Arabidopsis. Cold Spring Harb Protoc 2006: pdb.prot4668
Pubmed: Author and Title
CrossRef: Author and Title
Google Scholar: Author Only Title Only Author and Title

Willats WGT, McCartney L, Knox JP (2001) In-situ analysis of pectic polysaccharides in seed mucilage and at the root surface of Arabidopsis thaliana. Planta 213: 37-44
Pubmed: Author and Title
CrossRef: Author and Title
Google Scholar: Author Only Title Only Author and Title

Winter D, Vinegar B, Nahal H, Ammar R, Wilson G V., Provart NJ (2007) An "electronic fluorescent pictograph" Browser for exploring and analyzing large-scale biological data sets. PLoS One 2: e718
Pubmed: Author and Title
CrossRef: Author and Title
Google Scholar: Author Only Title Only Author and Title

Yin L, Verhertbruggen Y, Oikawa A, Manisseri C, Knierim B, Prak L, Jensen JK, Knox JP, Auer M, Willats WGT, et al (2011) The cooperative activities of CSLD2, CSLD3, and CSLD5 are required for normal Arabidopsis development. Mol Plant 4: 1024-37
Pubmed: Author and Title
CrossRef: Author and Title
Google Scholar: Author Only Title Only Author and Title

Yu L, Shi D, Li J, Kong Y, Yu Y, Chai G, Hu R, Wang J, Hahn MG, Zhou G (2014) CSLA2, a Glucomannan Synthase, is Involved in Maintaining Adherent Mucilage Structure in Arabidopsis Seed. Plant Physiol 164: 1842-1856
Pubmed: Author and Title
CrossRef: Author and Title
Google Scholar: Author Only Title Only Author and Title